Electrical Power and Energy Systems 156 (2024) 109719

Contents lists available at ScienceDirect

International Journal of Electrical Power and Energy Systems

journal homepage: www.elsevier.com/locate/ijepes

Review

Global optimization of economic load dispatch in large scale power systems using an enhanced social network search algorithm

Mohamed H. Hassan [a], Salah Kamel [b], Francisco Jurado [c,*], Umberto Desideri [d]

[a] Ministry of Electricity and Renewable Energy, Cairo, Egypt
[b] Department of Electrical Engineering, Faculty of Engineering, Aswan University, 81542 Aswan, Egypt
[c] Department of Electrical Engineering, University of Jaen, 23700 Jaén, Spain
[d] Department of Energy, Systems, Territory and Construction Engineering, University of Pisa, Pisa, Italy

ARTICLE INFO

Keywords:
Economic dispatch
Enhanced social network search
Power losses
Large scale power systems Valve point loading

ABSTRACT

The primary objective of Economic Load Dispatch (ELD) is to determine the most efficient distribution of power among generating units while considering various constraints, such as minimum and maximum power output, transmission line capacity, and reserve requirements. By solving the ELD problem, power system operators can minimize the overall operating cost of the power system and enhance its efficiency, which has far-reaching implications for sustainable energy management and resource allocation. However, because of the non-convex nature of the ELD problem, finding the global optimum solution poses a significant challenge. Consequently, several optimization techniques, such as metaheuristics, have been developed in order to address this type of problems. By iteratively exploring the solution space, metaheuristics offer a higher likelihood of finding near-optimal solutions, even in the presence of multiple local optima. This research introduces an enhanced social network search (ESNS) algorithm as an improvement over the existing social network search (SNS) algorithm, aiming to achieve the aforementioned objectives. The core of the SNS algorithm is driven by the social network users' dialogue, imitation, creativity, and disputation moods. The proposed ESNS algorithm builds upon the SNS approach by enhancing its search capability, particularly around the best potential solution. The primary goal is to improve the algorithm's ability to explore global search possibilities while avoiding being trapped in locally optimal solutions. The performance of ESNS has been tested in the 23 benchmark test suits, and its superiority against SNS and other recent algorithms has been verified. Moreover, To evaluate the effectiveness of the proposed ESNS algorithm, it is applied to four standard test systems comprising 11-, 15-, 40-, and 110-unit test systems. The results demonstrate that the ESNS algorithm outperforms other optimization algorithms in terms of solution quality and convergence speed. These findings suggest that the ESNS algorithm holds significant promise as a valuable tool for researchers and power system operators in addressing the economic dispatch problem. Overall, the ESNS technique presents a promising result to this complex challenges. Its capability to handle multiple constraints and its superior performance compared to other recent algorithms make it a valuable addition to the existing set of tools available for solving ELD.

1. Introduction

Economic Load Dispatch (ELD) plays a vital role in the economic operation of power systems. It involves the optimization of active power generation units to meet the system's total load demand while minimizing costs and adhering to various operational constraints [1]. ELD is an essential problem in power system economics as it helps utility companies and system operators make efficient power generation and allocation decisions. The primary objective of ELD is to allocate the optimal load generation to different power units within the system in order to minimize the overall generation costs. This involves determining the most cost-effective combination of power generation from different sources, such as thermal power plants, hydroelectric plants, and renewable energy sources [2]. By optimizing the generation schedule, ELD enables power system operators to strike a balance between meeting the electricity demand and minimizing production costs.

* Corresponding author.
E-mail addresses: mohamedhosnymoee@gmail.com (M.H. Hassan), skamel@aswu.edu.eg (S. Kamel), fjurado@ujaen.es (F. Jurado), umberto.desideri@unipi.it (U. Desideri).

https://doi.org/10.1016/j.ijepes.2023.109719
Received 13 June 2023; Received in revised form 13 November 2023; Accepted 8 December 2023
Available online 15 December 2023

ELD considers various constraints and factors that affect power generation, such as the capacity limits of each unit, transmission line losses, reserve requirements, and environmental considerations. These constraints ensure that the ELD solution is feasible and reliable in practical implementation [3].

Global optimization methods refer to algorithms and techniques designed to find the global optimum solution for the optimization problems. Global optimization seeks the best solution across the entire feasible solution space, considering all possible solutions. Common global optimization methods include genetic algorithms, simulated annealing, particle swarm optimization, ant colony optimization, differential evolution, and among others. The choice of method depends on the specific characteristics of the optimization problem.

Developing global optimization methods involves creating algorithms and techniques designed to find the optimal solution of an optimization problem across its entire solution space, rather than just a local optimum. Developing global optimization methods poses several challenges due to the complex nature of optimization problems and the need to find solutions that are not only locally optimal but also globally optimal. Addressing these challenges often involves a combination of heuristic techniques, metaheuristic algorithms, and intelligent strategies for balancing exploration and exploitation. It requires a deep understanding of the problem domain and careful consideration of the specific characteristics of the optimization problem at hand. Researchers continually strive to develop novel algorithms that can efficiently navigate complex, high-dimensional, and non-convex solution spaces to find globally optimal solutions.

The objective function of ELD aims to minimize the total generation cost, which includes fuel costs, start-up costs, and operational costs while satisfying the demand–supply balance. The field of ELD has witnessed extensive research and development, leading to the emergence of numerous optimization algorithms and computational techniques [4]. Various optimization techniques and algorithms have been developed, such as linear programming, quadratic programming, genetic algorithms, particle swarm optimization, and simulated annealing. These methods help in finding the optimal generation schedule that meets the load demand while considering the economic and operational constraints [1].

In recent years, various optimization algorithms have been extensively utilized to address the Economic Load Dispatch (ELD) problem. These algorithms aim to find the optimal solution for ELD by efficiently allocating and dispatching power generation units while considering the associated constraints and objectives. Among these algorithms, particle swarm optimization (PSO) [5] and its related techniques [6–9], teaching learning based optimization (TLBO) [10], weight-enhanced particle swarm optimization (WEPSO) [11], multigroup marine predator algorithm (MGMPA) [12], salp swarm algorithm (SSA) [13], backtracking search optimization (BSO) [14], improved slime mould algorithm (ISMA) [15], Chaotic slime mould algorithm (CSMA) [16], constrained cooperative adaptive multi-population differential evolutionary (CCAMDE) technique [17], artificial cooperative search (ACS) algorithm [18], evolutionary programming (EP) [19], ant lion optimizer (ALO) [20], one rank cuckoo search algorithm (ORCSA) [21], modified Symbiotic Organisms Search algorithm (MSOS) [22], oppositional real coded chemical reaction optimization (ORCCRO) [23], adaptive charged system search algorithm (ACSS) [24], chemical reaction optimization (CRO) [25], enhanced moth-flame optimizer (EMFO) [26], search group optimization (SGO) [27], Distributed auction optimization algorithm (DAOA) [28], Kho-Kho optimization (KKO) algorithm [29], Ameliorated grey wolf optimization algorithm (AGWO) [30], Indicator & crowding distance-based evolutionary algorithm [31], artificial cooperative search algorithm (ACS) [18], Colonial competitive differential evolution [32], Franklin's and Coulomb's laws theory optimizer (CFA) [33], and modified crow search algorithm (MCSA) [34] have been prominently employed.

Similarly, an eagle-strategy supply–demand-based optimization technique with chaotic (ESCSDO) improved using eagle strategy with ten chaotic maps [4]. its efficiency has been tested on ELD problems with four power systems. A clustering cuckoo search optimization (CCSO) algorithm was suggested to solve the ELD problem using a clustering mechanism to improve the searching balance between exploration and exploitation of each solution in [35]. The CCSO was applied on five different test systems, namely, 6 unit, 10 unit, 11 unit, 13 unit, 15 unit, and 40 unit systems by considering the constraints such as transmission losses and valve-point loading. In [36], the authors have enhanced the exploration and convergence capability of original TLBO by introducing the idea of quasi-oppositional-based learning to solve the ELD problem. In [37], a relative study of five soft computing algorithms, namely, differential evolution (DE), PSO, evolutionary programming (EP), genetic algorithm (GA), and simulated annealing (SA), was suggested for dynamic ELD problem by taking into consideration the constraints including generator ramp rate limits.

Despite the significant advantages, the addressed algorithms suffer from some drawbacks such as premature convergence and getting stuck in the local optimal points. One of the solutions to deal with these challenges and increase the accuracy and robustness of the algorithms is to modify, improve or hybridize them with other algorithms/methods [38]. The hybrid metaheuristics are the recent trend in the optimization domain and are heavily used for ELD due to their efficient optimization structure and powerful performance [39]. In The hybrid capuchin search algorithm with gradient search algorithm (CSGSA) algorithm, a memory element was added to this algorithm to ameliorate its position and velocity update mechanisms in order to exploit the most encouraging candidate solutions [40]. two adaptive parametric functions were used to manage the exploration and exploitation features of this algorithm and balance them appropriately. Several hybrid metaheuristics are proposed for ELD problems such as hybrid artificial algae algorithm [41], hybrid grey wolf optimizer (HGWO) [42], hybrid differential evolution [43], hybrid salp optimization algorithm [44], the adaptive simulated annealing (ASA) and genetic algorithms (GA) [45], hybrid DE and PSO techniques (DEPSO) [46], Greedy Randomized Adaptive Search Procedure (GRASP) algorithm and DE algorithm [47], Differential Evolution-Crossover Quantum Particle Swarm Optimization (DE-CQPSO) algorithm [48], etc.

These optimization algorithms provide efficient and effective means to handle the complexity of the ELD problem. By leveraging computational intelligence and search strategies inspired by natural phenomena, these algorithms explore the solution space and converge toward optimal or near-optimal solutions. They consider various factors, including generation costs, load demand, transmission constraints, and environmental factors, to achieve the best allocation and dispatch of generation units. The successful implementation of ELD can lead to significant benefits for power system operators, including reduced operating costs, improved fuel efficiency, enhanced system reliability, and a more sustainable energy mix. It also promotes the integration of renewable energy sources by optimizing their utilization and minimizing the reliance on fossil fuel-based generation.

Despite the extensive research conducted on different types of ELD problems, the inherent complexities of the search space demand the progress of more advanced optimization tools to attain highly optimal solutions. In this paper, particular attention is given to a non-convex continuous model of the ELD problem. This model incorporates the quadratic fuel cost of each generator, both with and without Valve Point Loading Effects (VPLEs). The problem is subject to power balance constraints and thermal generator limits, which reflect the limitations of the power system. The ELD problem is highly intricate, involving multiple variables and constraints. The objective is to minimize the overall fuel cost of power generation while fulfilling the demand for electrical load. However, due to non-convexities and the interplay of various factors, traditional optimization techniques may struggle to provide optimal or near-optimal solutions. Hence, there is a need for more sophisticated optimization tools that can effectively navigate the complex search space and consider the dynamic characteristics of power generation units. By developing improved optimization techniques, researchers aim to enhance the accuracy and efficiency of ELD solutions, leading to cost savings and improved operational performance in power systems.

In this study, the non-convex continuous model of the ELD problem is addressed, taking into account the quadratic fuel cost function and considering the power balance and thermal generator limitations. By formulating the problem in this manner, researchers can explore advanced optimization methods that can handle the non-linear and non-convex nature of the ELD problem more effectively. The development of better optimization tools for the ELD problem is crucial for power system operators and planners to make informed decisions regarding the allocation and dispatch of power generation resources. By achieving more optimal solutions, it becomes possible to minimize fuel costs, improve the economic efficiency of power generation, and ensure the reliable and stable operation of the power system. By addressing the complexities of the ELD problem and developing more advanced optimization techniques, this research aims to contribute to the optimization and economic efficiency of power systems. It strives to enhance the understanding of the ELD problem and provide valuable insights that can drive improvements in power system operation and planning.

According to the 'No free lunch theorems for optimization,' it is not feasible to determine which optimization technique will consistently achieve the global optimum for all optimization problems [49 50]. Recently, a novel optimization technique called the Social Network Search (SNS) has been introduced [51]. This algorithm draws inspiration from the social network users' dialogue, imitation, creativity, and disputation moods. The original SNS technique demonstrates fast convergence due to its ease of implementation and strong adaptability. Its results showed that it is capable of outperforming various methods in dealing with different optimization problems [51]. Because of its benefits as a robust metaheuristic algorithm, it was applied to solve several optimization problems such as optimal power system operation problem and applied on an IEEE standardized 57-bus power system and real Egyptian power system of the West Delta area [52], reliability improvement-based reconfiguration of distribution networks [53], and 14 benchmark engineering optimization problems and one real application in the field of remote sensing [54]. According to [55], the SNS algorithm was used for OPF in its traditional configuration, but its related reliability required additional support and adaptations in the fields of power simulations and optimizations, mathematical benchmarking frameworks, and complex engineering challenges. Also, once it becomes trapped in a local optimum, escaping from the local minima becomes exceedingly difficult. To address this issue, the SNS algorithm incorporates concepts from high and low-velocity ratios strategy. These suggested modifications not only improve the SNS's ability to balance exploitation and exploration but also enhance its capacity to explore solutions more effectively. The primary objective of global optimization is to create an enhanced version of SNS that improves its exploration capabilities.

The proposed technique, known as the Enhanced Social Network Search (ESNS), leverages the “High and Low-Velocity Ratios” to achieve the optimal solution for the objective function. This article employs the ESNS method to solve the ELD problem to showcase its effectiveness in solving nonlinear optimization problems. The utilization of the ESNS in tackling the ELD problem is motivated by the desire to employ a highly effective and efficient optimization technique. The ELD problem poses significant challenges due to its complexity, characterized by multiple constraints, non-convexity, and nonlinearity. These complexities make it essential to explore advanced optimization algorithms to obtain optimal or near-optimal solutions for the ELD problem. The research presented in this study focuses on the following key contributions:

- The research introduces and develops the ESNS algorithm, inspired by the social network users' dialogue, imitation, creativity, and disputation moods. The ESNS algorithm is designed to address complex optimization problems and offers a novel approach for finding optimal or near-best solutions.
- The ESNS technique is thoroughly tested and confirmed against 23 benchmark functions commonly used in optimization research. This step ensures that the algorithm performs reliably and effectively, providing a solid foundation for its application in practical problems.
- The research demonstrates the efficiency of the ESNS approach through evaluating its performance against various benchmark functions. The results highlight the algorithm's capability to converge towards optimal solutions efficiently, showcasing its efficacy as an optimization technique.
- To validate the effect of the ESNS technique, the ESNS results were compared with those of the SNS, MPA, WHO, EO, JS and ARO algorithms.
- The study extends the application of the ESNS algorithm to tackle the ELD problem, which is a complex optimization problem with multiple constraints and nonlinearity. By utilizing the ESNS algorithm, the research aims to optimize the allocation and dispatch of power generation units, considering the system's load demand and operational constraints.
- To assess the resilience and solution quality of the ESNS algorithm, the research compares its performance with comparable approaches from the existing literature. By conducting simulation experiments and analyzing the results, the study provides insights into the advantages and competitiveness of the developed ESNS algorithm.

These contributions collectively advance the field of optimization by introducing the ESNS algorithm, validating its performance, applying it to the ELD problem, and evaluating its effectiveness against existing approaches. The research provides valuable insights and establishes the ESNS algorithm as a promising optimization technique for solving complex real-world problems.

The research study encompasses the following sections: In Section 2, the mathematical formulation of the Economic Load Dispatch (ELD) problem is presented. This section defines the objective function and constraints that govern the allocation and dispatch of power generation units in the ELD problem. Section 3 provides a comprehensive explanation of the Enhanced a Social Network Search (ESNS) technique. The algorithm's key components, such as initialization, search operators, and termination criteria, are described in detail to provide a clear understanding of how the ESNS algorithm operates. Section 4 presents the findings and discussions resulting from the application of the developed ESNS algorithm to solve the ELD problem. The performance of the proposed ESNS algorithm is evaluated based on various metrics, and the results are analyzed and discussed in the context of optimizing the allocation and dispatch of power generation units. Section 5 presents the discussion of the simulation results. Finally, in Section 6, the research concludes with a summary of the key findings and contributions.

2. Formulation of economic load dispatch problem

The objective of the ELD problem is to determine the optimal power outputs of thermal generation unit across different operational zones in an electricity network. This optimization aims to reduce the overall fuel cost while ensuring that the system and generating units operate within their respective limitations. In the context of ELD, various constraints need to be considered, such as power balance while accounting for transmission line losses, limits on generating capacity, valve-point loading effects, restrictions on ramp rates, and prohibited operating zones (POZs). The fitness function, denoted as F_T, represents the non-convex cost function associated with the dedicated generating units [56].

$$F_T = \sum_{u=1}^{N} F_u(P_u) \tag{1}$$

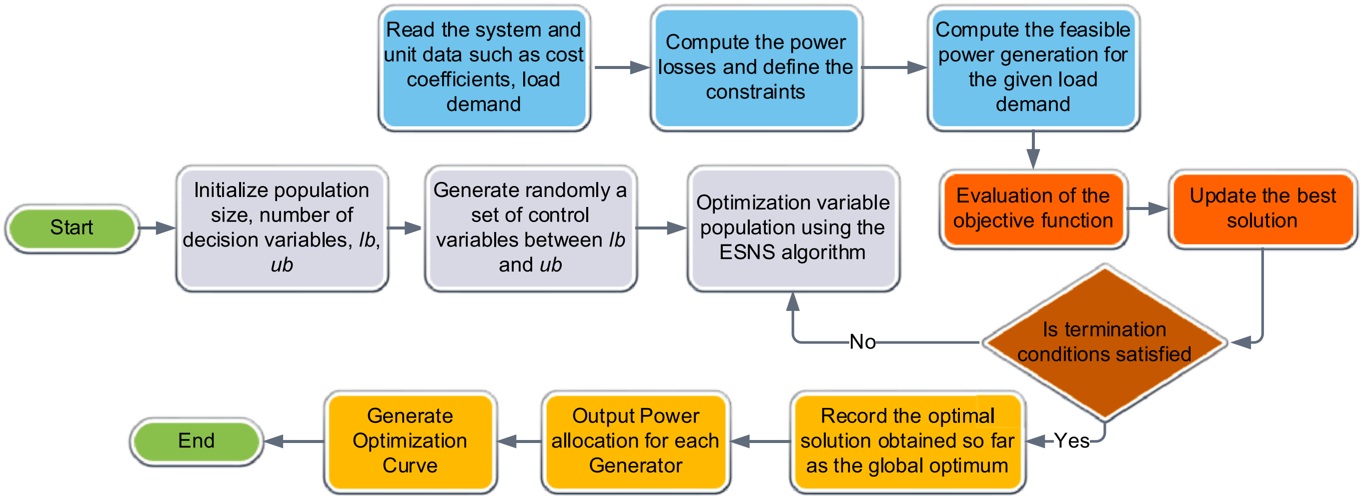

Fig. 1. The flowchart of ESNS for the ELD problem.

where the total cost of production is F_T, P_u is the u th unit generation, N is the number of dispatch able units.

(1) Smooth Cost Function Characteristics

Typically, the fitness function F_u for a thermal unit u is expressed by Equation (2) [15].

$$F_u(P_u) = a_u + b_u P_u + c_u P_u^2 \tag{2}$$

where a_u, b_u, and c_u denote the input fuel coefficients of scheduled units. P_u refers to the output power of the u^{th} committed unit.

(2) Nonsmooth Cost Function Characteristics

The fuel cost function of thermal power stations incorporates non-convexity due to the effect of steam valve opening. Each thermal power station is equipped with a specific valve opening system that regulates the flow of superheated dry steam to the turbine units. When these valves are activated, a slight reduction in power output occurs, resulting in fluctuations in the fitness function curve. This phenomenon, known as the valve-point loading effect (VPLE), leads to an upward shift in the fuel cost curve. Mathematically, the VPLE can be described as follows [15]:

$$F_u(P_u) = a_u + b_u P_u + c_u P_u^2 + \left| d_u \sin\left(e_u \left(P_{u,min} - P_u\right)\right) \right| \tag{3}$$

where d_u and e_u represent the unit u cost coefficients, and $P_{u,min}$ denotes the minimum generated power.

(3) Constraints for ELD problem
- Power balance criterion

The ELD problem involves several constraints, including power balance constraints, power loss constraints, and other common requirements such as generation capability limits and active power balance constraints. These constraints can be expressed as follows:

$$0 = \sum_{u=1}^{n} P_u - P_L - P_D \tag{4}$$

Where P_D is the total demand. The transmission line losses (P_L) in the ELD problem are calculated using Kron's formula, which is given by:

$$P_L = \sum_{u=1}^{n} \sum_{j=1}^{n} P_i B_{ij} P_j + \sum_{i=1}^{n} B_{0i} P_i + B_{00} \tag{5}$$

where B_{ij}, B_{0i}, B_{00} are the B-matrix coefficients for P_L, which can be generally assumed to be constants under a normal operating condition.

- **Generating capacity constraint**

To ensure that the power output P_u of each unit falls within the minimum and maximum power generation limits, the following condition is applied [57]:

$$P_u^{min} \le P_u \le P_u^{max} \tag{6}$$

where P_u^{max} denotes maximum bound for the u th unit.

- **Ramp rate constraint**

In real scenarios, the output power P_u of a generation unit cannot be adjusted instantaneously due to the operating limit imposed by its ramp rate. This means that the power adjustment is subject to the following up and down ramp limits:

$$P_u - P_u^0 \le UR_u and P_u^0 - P_u \le DR_u \tag{7}$$

The current power output, denoted as P_u, is determined based on the previous power output, P_u^0, while considering the up limit (UR_u) and down bound (DR_u) of u th unit.

From these Equations (6)–(7) the output power is defined from the following equation:

$$\max(P_u^{min}, P_u^0 - DR_u) \le P_u \le \min(P_u^{max}, P_u^0 + UR_u) \tag{8}$$

- **Prohibited operating zones (POZs)**

In applied operation, the availability of the complete operating zones of a generator is often restricted due to physical constraints. These restrictions result in discontinuous regions for the objective function. These constrained regions, known as Prohibited Operating Zones (POZs), arise due to factors such as shaft-bearing vibrations caused by steam valves or ancillary equipment like boilers or feed pumps. To ensure proper operation, the output power P_u of a generator must satisfy the following constraints related to POZs:

$$\begin{aligned} P_u^{min} &\le P_u \le P_{u,1}^{l} \\ P_{u,k-1}^{up} &\le P_u \le P_{u,k}^{l}, k = 2, \cdots\cdots, p_{zu} \\ P_{u,pz_u}^{up} &\le P_u \le P_{u,1}^{max} \end{aligned} \quad (9)$$

where $P_{u,k}^{l}$ and $P_{u,k}^{up}$ refer to the lower and upper bounds of the *kth* prohibited zone of unit u, respectively, k denotes the index of POZs (pz_u).

- **Constraint handling technique**

In addressing the challenge of constraint infringement within this ELD problem, a methodology based on a penalty function has been employed [36]. Within this framework, static penalty functions are harnessed to calculate the penalized generation cost associated with solutions that do not conform to the set constraints. The cumulative generation cost is determined as follows:

$$F(P) = F_u(P_u) + \sum_{h=1}^{l} \mu_h \times \max[0, r_h(P_u)]^2 + \sum_{m=1}^{n} \lambda_m \times \max[0, s_m(P_u)]^2 \quad (10)$$

where l denotes the count of inequality constraints ($r_h(P_u) \ge 0$) and n represents the quantity of equality constraints ($s_m(P_u) = 0$), the static penalty coefficients are μ_h and λ_m. In general, high values of penalty coefficients are considered. Hence, the objective at hand is to minimize equation (10), while taking into account either cost function (2) or (3), subject to the proposed optimization technique and the presence of both equality constraints (4) and inequality constraints (6–8). Fig. 1 shows the flowchart of the ELD optimization performed by the proposed ESNS technique. In Fig. 1, the flowchart illustrates the intricate steps involved in the Economic Load Dispatch optimization process by the proposed ESNS technique. The flowchart presents a sequence of operations to how the ELD be solved by the ESNS method toward achieving optimal power generation distribution within a power system.

3. The proposed enhanced social network search

(1) Social Network Search algorithm

The Social Network Search (SNS) technique replicates the behavior of operators in social networks, where they strive to gain status by expressing their opinions. This technique incorporates the moods of users, namely imitation, conversation, disputation, and innovation, which are observed in real-world community link interactions. The mathematical representation of these moods is as below:

(a) Imitation

$$\begin{aligned} X_{i,new} &= X_j + rand(-1,1) \times M \\ R &= rand(0,1) \times h \\ h &= X_j - X_i \end{aligned} \quad (11)$$

Where, X_j refers to the the jth user's view's vector that is selected by random and $i \ne j$ and X_i denotes the vector of the ith user's view. The shock radius (R) reflects the amount of influence of the jth user, and its magnitude is considered as a multiple of h.

(b) Conversation

$$\begin{aligned} X_{i,new} &= X_k + M \\ R &= rand(0,1) \times B \\ B &= sign(f_i - f_j) \times (X_j - X_i) \end{aligned} \quad (12)$$

Where, X_k represents the vector of the issue that is selected by random to speak about it. B is the difference between the views of users and it is no parameters for such computation of difference among views.

(c) Disputation

$$\begin{aligned} X_{i,new} &= X_i + rand(0,1) \times (G - AF \times X_i) \\ G &= \frac{\sum_t^{N_r} X_t}{N_r} \\ AF &= 1 + round(rand) \end{aligned} \quad (13)$$

Where, X_i denotes the vector of the view of the *ith* user and G proves the mean of the users' views in the group. AF represents the admission factor. N_r denotes the group size.

(d) Innovation

$$\begin{aligned} X_{i,new}^{d} &= \mathrm{t} \times X_j^d + (1 - \mathrm{t}) \times n_{new}^{d} \\ n_{new}^{d} &= lb + rand_1 \times (ub - lb) \\ t &= rand_2 \end{aligned} \quad (14)$$

Where, d is the *dth* variable that is selected randomly in the interval of the variables of the problem. n_{new}^d denotes the new idea while x_j^d represents the current idea.

This procedure is displayed as below:

$$X_{i,new} = [x_1, x_2, x_3, \cdots\cdots x_{i,new}^{d} \cdots\cdots x_D] \quad (15)$$

In order to discovery the value of new view, the objective functions of $X_{i,new}$ and X_i should be computed and then compare between them and the new value of X_i is computed as follows:

$$X_i = \begin{cases} X_i, f(X_i) < f(X_{i,new}) \\ X_{i,new}, f(X_{i,new}) \ge f(X_i) \end{cases} \quad (16)$$

(2) *Enhanced Social network search (ESNS)*.

The high and low-velocity ratio approach, known as the Marine Predator Algorithm (MPA) [58], has been devised to address the problem of potential optimum values getting trapped in local optima. This adaptation consists of two stages, starting with the high-velocity ratio scenario. The model for this stage is outlined below:

$$iter < \frac{1}{3} MaxIt \quad (17.1)$$

$$S = \overrightarrow{R_B} \otimes \left(E - \overrightarrow{R_B} \otimes X_i(t)\right) \quad (17.2)$$

$$X_i(t+1) = X_i(t) + P.\overrightarrow{R_B} \otimes S \quad (17.3)$$

Through the initial third of iterations, while a large step size indicates a high level of investigative capability, the fittest solution (E) is identified as the superlative position. This position is then utilized to construct a matrix using the following process:

where $\overrightarrow{R_B}$ represents a vector consisting of random integers, reflecting Brownian motion. The notation $\otimes$ signifies entry-by-entry multiplications. $P = 0.5$ represents a constant value. $\overrightarrow{R_B}$ is a vector composed of uniform random values within the range [0,1]. The new location is simulated by multiplying $\overrightarrow{R_B}$ with the preceding location, incorporating the constant value P, and the element-wise product $\otimes$ operation. This generates the matrix formulation as follows:

$$E = \begin{bmatrix} Xb_{1.1}^{t} & \cdots & Xb_{1.d}^{t} \\ \vdots & \ddots & \vdots \\ Xb_{n.1}^{t} & \cdots & Xb_{n.d}^{t} \end{bmatrix} \quad (18)$$

In the second stage, known as the low-velocity ratio, which typically happens towards the end of the optimization procedure, considered by a high exploitation capability, the Lévy distribution is considered the most

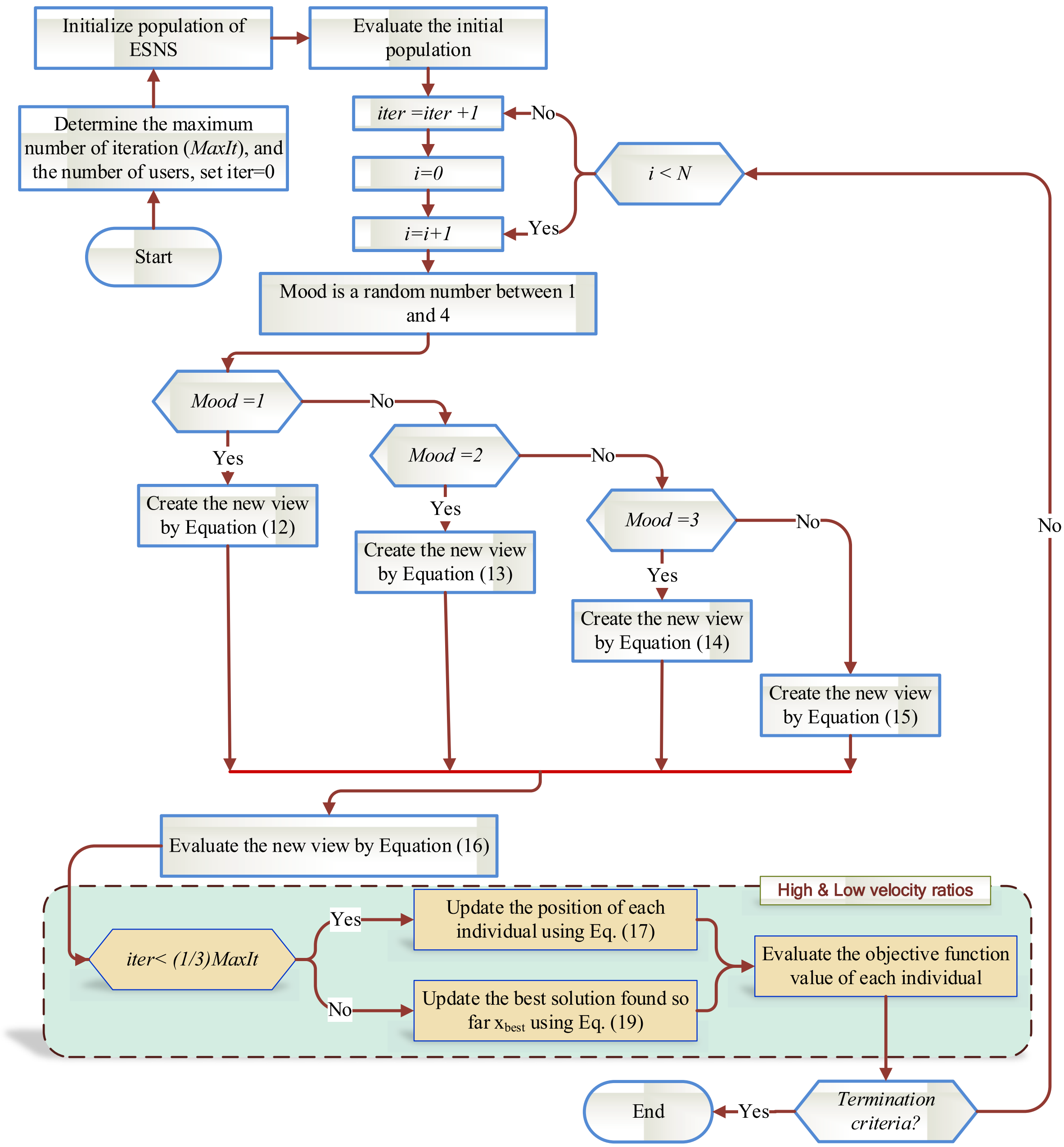

Fig. 2. The flowchart of the ESNS technique.

effective approach. This stage can be described as follows:

where *Xb* represent the best solution that is duplicated n times to form the E matrix. Here, n refers to the number of population, while d represents the number of dimensions. During the low-velocity ratio stage, the Lévy distribution is utilized to guide the search agents toward refined solutions. This distribution helps in achieving a balance between exploration and exploitation. The specific implementation and mathematical model for this stage may vary depending on the context and the specific details of the optimization algorithm being employed.

$$iter > \frac{1}{3}MaxIt \tag{19.1}$$

$$S = \overrightarrow{R_L} \otimes \left(\overrightarrow{R_L} \otimes E - X_i(t) \right) \tag{19.2}$$

$$X_i(t+1) = E + P.CF \otimes S \tag{19.3}$$

The Lévy method is employed in the proposed algorithm, where the multiplication of R_L and E, along with the addition of the step size to the location, facilitates the update of the position. *CF* is considered as an adaptive parameter to control the step size. This technique not only updates the position but also increases the likelihood of escaping from local minima, enhancing the exploration capability of the ESNS algorithm. Fig. 2 displays the flowchart of the ESNS technique, showcasing the incorporation of high and low-velocity ratios inside the technique. This amendment plays a crucial role in boosting the exploration aspect of the proposed ESNS algorithm, allowing for a more comprehensive search of the solution space. Moreover, Algorithm 1 describes the ESNS algorithm's pseudocode.

Algorithm 1: Pseudocode of the ESNS algorithm

Set the control parameter (Dimension of problem (d), maximum iteration, population size), lower bounds (lb) and upper bounds (ub)

(*continued on next page*)

(*continued*)

Algorithm 1: Pseudocode of the ESNS algorithm

```
    Initialize the population randomly
    Evaluate the fitness of the new solution
    Extract the best solution
    While iter ≤ MaxIt
    Randomly generate Mood as an integer value from range 1 to 4.
    For i = 1:N
      If Mood = 1
        Apply the imitation model to create the new view by Eq. (12)
      Else If Mood = 2
        Apply the conversation model to create the new view by Eq. (13)
      Else If Mood = 3
        Apply the disputation model to create the new view by Eq. (14)
      Else If Mood = 4
        Apply the innovation model to create the new view by Eq. (15)
End If
End For
    Check the limits of the new locations and evaluate the fitness values by Eq. (16)
    % high and low-velocity ratio approach
For i = 1:N
      If iter < 1/3 MaxIt
        Update the new location of the each individual using Eq.(17)
      Else If
        Update the new location of the each individual using Eq.(19)
End If
End For
    Check the limits of the new locations and evaluate the fitness values
    Find the new solution if the fitness is better
    iter = iter + 1
    End while
    Output the best solution
```

(3) Analysis of Algorithm Computational Complexity

The time complexity of the proposed ESNS technique is contingent on the number of search agents (N), the maximum number of iterations (T), and the problem's dimensions (D). In the original SNS, the time complexity for initializing the population is O (N x D). At each iteration, the time complexity for updating locations of the four moods (imitation model, conversation model, disputation model, and innovation model) is O (Nx D x T). Therefore, the overall time complexity of SNS can be expressed O (N x D x T + Nx D). For ESNS, the time complexity for updating locations of high and low-velocity ratio is O (Nx D x T). Consequently, the overall time complexity of ESNS is O (2 x N x D x T + Nx D).

4. Simulation results and discussion

4.1. Benchmark functions

In this study, the evaluation focuses on the performance of different algorithms on benchmark functions F1-F13. The experiments were conducted in thirty-dimensions using number of population is 50 and number of maximum iteration is 200 for the whole methods. The parameter settings of the optimization techniques are shown in Table 1. All simulations have been implemented on a laptop, including Core i5-4210U CPU@ 2.40 GHz of speed and 8 GB of RAM. The MATLAB 2016a platform was used to execute the techniques.

The statistical results of 23 benchmark functions obtained by the ESNS technique and other recent algorithms, including wild horse optimizer (WHO) [59], Equilibrium optimizer (EO) [60], jellyfish search optimizer (JS) [61], and artificial rabbit algorithm (ARO) [62], as well as the original SNS and MPA [58], are presented in Table 2. The proposed ESNS technique exhibits exceptional performance, outperforming other algorithms in 13 out of the 23 functions. It achieves the lowest function values and attains the highest rank in these cases. The results indicate that the ESNS algorithm surpasses other algorithms in terms of best, median, worst, mean, and standard deviation (STD) values for most of the functions. Especially, ESNS demonstrates superior performance in functions F1, F2, F4, F6, F8, F9, F10, F11, F12, F14, F16, F17, and F19 showing significant differences compared to other methods in both best and average values, while maintaining a very small standard deviation.

Table 1
Parameter settings of optimization techniques.

Algorithm	Parameter settings
WHO	*PC = 0.13, PS = 0.2*
GWO	*a = Linear reduction from 2 to 0*
GBO	*FADs = 0.2, Pr = 0.5*

Overall, Table 2 consistently demonstrates the superior performance of the ESNS technique compared to other recent algorithms in solving the benchmark functions. These results highlight the effectiveness and efficiency of the ESNS technique in addressing optimization problems. Moreover, the ESNS algorithm exhibits the lowest standard deviation, indicating high consistency across different runs. The favorable ranking of the ESNS technique in this study suggests its potential as a promising optimization method for various real-world applications.

Fig. 3 shows a radar chart for the ranking of all compared algorithms for each function. The average of these ranks is presented in Fig. 4. In this Figure, it can be seen that ESNS has the lowest average rank value, implying that it ranks first among all algorithms. This underscores ESNS as the top-performing algorithm in the comparison, based on the tied rank method. This outcome further confirms that our technique can competently discover the global optimal for several problems.

The efficacy of the proposed ESNS algorithm is demonstrated through an extensive analysis of its performance on twenty-three benchmark functions. The convergence curves of various optimization techniques, including ESNS, have been plotted in Fig. 5, highlighting the outstanding performance of the ESNS technique in comparison to the others. This graphical representation clearly showcases the superiority of ESNS in terms of convergence rate and solution quality.

In order to gain deeper insights into the performance of the suggested ESNS algorithm, a comprehensive evaluation is conducted by presenting a boxplot of outcomes for each optimization algorithm and objective function in Fig. 5. The boxplot provides a visual summary of the distribution and characteristics of the performance metrics for each algorithm. By analyzing these boxplots, it becomes evident that the ESNS algorithm consistently outperforms the other techniques across all objective functions.

These empirical findings provide compelling evidence to support the claim that the ESNS algorithm is highly effective in finding the optimal solution for the high-dimensional optimization problems. The superiority of ESNS is demonstrated not only through the convergence curves but also through the comprehensive analysis of performance metrics using the boxplot representation. The consistent and superior performance of ESNS on diverse benchmark functions reaffirms its capability to tackle complex optimization challenges efficiently.

Overall, the convergence curves in Fig. 5 and the boxplot analysis in Fig. 6 collectively confirm the efficacy of the ESNS algorithm, establishing it as a powerful and reliable optimization method for high-dimensional problems.

4.2. A. Wilcoxon's rank test results

In this subsection, the differences between ESNS and other algorithms are further analyzed statistically using the Wilcoxon rank-sum test (WRST), which is a paired test that checks for significant differences between two algorithms. The results of the test between ESNS and each technique at a significance level of α = 0.05 are presented in Table 3, where the symbols "+/=/-" show whether ESNS executes better, similarly, or worse than the comparison technique. This Table also presents the statistical results of ESNS in different dimensions and functions, signifying whether ESNS performs better, similarly, or worse

Table 2
The statistical Results of 23 benchmark functions by the ESNS algorithms and other recent algorithms.

Function		ESNS	SNS	MPA	WHO	EO	JS	ARO
F1	Best	6.57E−33	1.03E−28	1.68E−07	5.08E−21	2.38E−18	6.48E−15	1.59E−26
	Average	7.24E−32	1.37E−27	5.11E−07	2.85E−18	1.69E−17	7.73E−12	1.07E−21
	Median	5.02E−32	4.77E−28	3.6E−07	1.14E−18	1.09E−17	5.7E−13	4.68E−23
	Worst	3.77E−31	1.04E−26	1.81E−06	1.11E−17	6.39E−17	1.22E−10	7.08E−21
	std	8.98E−32	2.38E−27	4.1E−07	3.57E−18	1.72E−17	2.71E−11	2.18E−21
—	Rank	1	2	7	4	5	6	3
F2	Best	4.55E−17	2.3E−15	2.28E−05	4.13E−13	5.21E−11	1.13E−07	1.34E−14
	Average	2.72E−16	5.64E−15	0.000156	1.3E−10	1.63E−10	3.31E−06	1.15E−12
	Median	2.09E−16	4.21E−15	0.000135	5.29E−11	1.42E−10	1.5E−06	1.22E−13
	Worst	8.32E−16	1.4E−14	0.00043	6.34E−10	4.47E−10	1.67E−05	1.78E−11
	std	2.06E−16	3.51E−15	9.51E−05	1.77E−10	1.03E−10	4.46E−06	3.94E−12
	Rank	1	2	7	4	5	6	3
F3	Best	2.67E−16	9.18E−13	0.274034	5.13E−13	7.16E−05	0.043236	4.28E−21
	Average	6.85E−15	4.18E−08	3.940563	1.2E−08	0.012312	37.7777	5.08E−15
	Median	3.29E−15	4.13E−09	3.263723	6.29E−11	0.001321	2.63887	6.99E−17
	Worst	2.79E−14	3.9E−07	8.369983	2.3E−07	0.149211	289.5644	6.41E−14
	std	8.32E−15	9.17E−08	2.31658	5.14E−08	0.034853	76.37593	1.51E−14
	Rank	2	4	6	3	5	7	1
F4	Best	1.58E−15	1.33E−13	0.001671	5.11E−09	1.78E−05	1.66E−08	8.35E−13
	Average	4.69E−15	5.45E−13	0.003476	3.5E−07	0.000138	2.28E−07	2.6E−09
	Median	3.68E−15	4.09E−13	0.003057	1E−07	5.67E−05	1.66E−07	7.79E−10
	Worst	1.14E−14	1.87E−12	0.006615	2.14E−06	0.000648	7.36E−07	2.28E−08
	std	2.89E−15	4.55E−13	0.001289	6.09E−07	0.000166	1.78E−07	5.09E−09
	Rank	1	2	7	5	6	4	3
F5	Best	25.35792	27.6644	25.94347	26.68451	25.6266	0.042193	0.048127
	Average	25.77146	28.03399	26.61776	37.10656	26.26018	0.654502	2.57084
	Median	25.74567	27.97984	26.70742	27.67985	26.11165	0.458008	1.069097
	Worst	26.33112	28.44604	27.5016	208.5133	27.83945	2.763539	16.26736
	std	0.234412	0.216873	0.397519	40.37046	0.498931	0.735235	3.783419
	Rank	3	6	5	7	4	1	2
F6	Best	3.36E−07	0.080879	0.011749	0.013248	0.000201	9.87E−07	0.009568
	Average	6.98E−07	0.292241	0.068693	0.064784	0.000497	2.02E−05	0.044563
	Median	6.17E−07	0.255115	0.063854	0.058665	0.000417	1.68E−05	0.039666
	Worst	1.53E−06	0.75842	0.15925	0.16971	0.001518	6.11E−05	0.098375
	std	3.17E−07	0.181696	0.037548	0.043941	0.000297	1.86E−05	0.026373
	Rank	1	7	6	5	3	2	4
F7	Best	7.71E−05	0.000168	0.000655	0.000605	0.000243	0.000288	3.22E−05
	Average	0.000734	0.000708	0.002961	0.001779	0.001908	0.001159	0.001407
	Median	0.000627	0.000688	0.00246	0.001387	0.001826	0.000994	0.00115
	Worst	0.002121	0.002187	0.006116	0.004938	0.005511	0.00267	0.003564
	std	0.000532	0.000488	0.001753	0.001255	0.001275	0.000648	0.001071
	Rank	2	1	7	5	6	3	4
F8	Best	−12086.2	−7613.49	−9098.32	−1807.46	−1796.54	−1909.05	−9902.5
	Average	−11651	−6358.62	−8329.76	−1721.44	−1743.05	−1904.86	−9268.23
	Median	−11631.3	−6324.46	−8346.16	−1729.69	−1742.67	−1909.01	−9276.94
	Worst	−11199.9	−5562.96	−7695.47	−1630.81	−1681.91	−1827.1	−7798.04
	std	230.5318	538.2484	401.4317	54.13894	28.37994	18.30237	494.4779
	Rank	1	4	3	7	6	5	2
F9	Best	0	0	4.32E−07	0	5.68E−14	0.000364	0
	Average	0	0	0.000143	1.11E−05	0.049752	0.089437	0
	Median	0	0	2.99E−05	1E−09	1.14E−13	0.058094	0
	Worst	0	0	0.001393	0.000177	0.99503	0.411201	0
	std	0	0	0.000307	3.96E−05	0.222496	0.113678	0
	Rank	1	1	5	4	6	7	1
F10	Best	4.44E−15	4.44E−15	4.93E−05	8.88E−16	20	0.108639	3.29E−14
	Average	4.44E−15	7.46E−15	0.000141	1.003597	20.00003	5.161577	5.19E−12
	Median	4.44E−15	6.22E−15	0.000119	7.99E−06	20	2.943275	1.26E−12
	Worst	4.44E−15	1.51E−14	0.000373	20.01369	20.00065	21.14854	5.25E−11
	std	0	3.69E−15	7E−05	4.474524	0.000145	6.667606	1.17E−11
	Rank	1	2	4	5	7	6	3
F11	Best	0	0	2.56E−07	0	0	0	0
	Average	0	0	1.83E−06	1.83E−16	1.39E−16	6.49E−13	0
	Median	0	0	1.37E−06	0	0	1.67E−16	0
	Worst	0	0	5.92E−06	3.66E−15	2.22E−15	1.21E−11	0
	std	0	0	1.56E−06	8.19E−16	4.92E−16	2.69E−12	0
	Rank	1	1	7	5	4	6	1
F12	Best	4.3E−08	0.000696	0.000793	4.64E−05	5.41E−06	1.88E−08	0.000211
	Average	9.48E−08	0.00268	0.00381	0.026544	1.46E−05	1.98E−07	0.002555
	Median	8.41E−08	0.00284	0.001677	0.000309	1.46E−05	1.74E−07	0.002594
	Worst	1.91E−07	0.004893	0.01777	0.207386	3.77E−05	6.76E−07	0.004551
	std	4.35E−08	0.001232	0.004928	0.056802	8.5E−06	1.59E−07	0.001218
	Rank	1	5	6	7	3	2	4
F13	Best	5.87E−07	0.057519	0.032728	0.011802	0.000219	8.24E−08	0.005253
	Average	0.002159	0.154385	0.09402	0.173897	0.039624	4.69E−06	0.038605

(continued on next page)

Table 2 (*continued*)

Function		ESNS	SNS	MPA	WHO	EO	JS	ARO
	Median	3.02E−06	0.140323	0.08078	0.136817	0.001307	3.52E−06	0.020631
	Worst	0.017656	0.378672	0.336438	0.700833	0.207579	1.58E−05	0.218513
	std	0.005029	0.077659	0.072531	0.157716	0.072678	4.12E−06	0.051532
	Rank	2	6	5	7	4	1	3
F14	Best	0.998004	0.998004	0.998004	0.998004	0.998004	0.998004	0.998004
	Average	0.998004	0.998004	0.998004	1.097209	0.998004	0.998004	0.998004
	Median	0.998004	0.998004	0.998004	0.998004	0.998004	0.998004	0.998004
	Worst	0.998004	0.998004	0.998004	2.982105	0.998004	0.998004	0.998004
	std	5.09E−17	1.02E−16	5.07E−16	0.443659	1.84E−16	2.55E−16	2.97E−16
	Rank	1	1	6	7	1	1	5
F15	Best	0.000307	0.000308	0.000307	0.000307	0.000308	0.000307	0.000308
	Average	0.000522	0.00035	0.00031	0.000602	0.004398	0.000316	0.000441
	Median	0.000308	0.000313	0.000307	0.000593	0.00035	0.000309	0.000404
	Worst	0.001594	0.000582	0.000332	0.001223	0.020363	0.000391	0.000694
	std	0.000415	6.8E−05	6.09E−06	0.000286	0.008192	1.92E−05	0.000131
	Rank	5	3	1	6	7	2	4
F16	Best	−1.03163	−1.03163	−1.03163	−1.03163	−1.03163	−1.03163	−1.03163
	Average	−1.03163	−1.03163	−1.03163	−1.03163	−1.03163	−1.03163	−1.03163
	Median	−1.03163	−1.03163	−1.03163	−1.03163	−1.03163	−1.03163	−1.03163
	Worst	−1.03163	−1.03163	−1.03163	−1.03163	−1.03163	−1.03163	−1.03163
	std	2.22E−16	1.53E−16	1.61E−14	5.09E−17	1.76E−16	1.97E−16	2.5E−12
	Rank	1	1	6	1	1	1	7
F17	Best	0.397887	0.397887	0.397887	0.397887	0.397887	0.397887	0.397887
	Average	0.397887	0.397887	0.397887	0.397887	0.397887	0.397887	0.397887
	Median	0.397887	0.397887	0.397887	0.397887	0.397887	0.397887	0.397887
	Worst	0.397887	0.397887	0.397887	0.397887	0.397887	0.397887	0.397887
	std	0	0	1.01E−12	0	0	0	1.28E−10
	Rank	1	1	6	1	1	1	7
F18	Best	3	3	3	3	3	3	3
	Average	3	3	3	3	3	3	3
	Median	3	3	3	3	3	3	3
	Worst	3	3	3	3	3	3	3
	std	1.26E−15	1.6E−15	1.53E−13	1.13E−15	2.16E−15	1.61E−15	1.16E−15
	Rank	2	5	7	1	5	2	2
F19	Best	−3.86278	−3.86278	−3.86278	−0.30048	−0.30048	−0.30048	−3.86278
	Average	−3.86278	−3.86278	−3.86278	−0.30048	−0.30048	−0.30048	−3.86278
	Median	−3.86278	−3.86278	−3.86278	−0.30048	−0.30048	−0.30048	−3.86278
	Worst	−3.86278	−3.86278	−3.86278	−0.30048	−0.30048	−0.30048	−3.86278
	std	2.24E−15	2.22E−15	2.77E−11	1.14E−16	1.14E−16	1.4E−09	3.73E−15
	Rank	1	1	4	5	5	7	3
F20	Best	−3.322	−3.322	−3.322	−3.322	−3.322	−3.322	−3.322
	Average	−3.26849	−3.29822	−3.322	−3.21756	−3.20051	−3.30416	−3.31597
	Median	−3.322	−3.322	−3.322	−3.322	−3.322	−3.322	−3.322
	Worst	−3.2031	−3.2031	−3.322	−2.43178	−1.84092	−3.2031	−3.2031
	std	0.060685	0.048793	2.27E−10	0.239908	0.327557	0.043556	0.026567
	Rank	5	4	1	6	7	3	2
F21	Best	−10.1532	−10.1532	−10.1532	−10.1532	−10.1532	−10.1532	−10.1532
	Average	−6.78631	−10.1532	−10.1532	−9.77706	−9.26724	−10.1532	−10.1187
	Median	−10.1532	−10.1532	−10.1532	−10.1532	−10.1532	−10.1532	−10.1532
	Worst	−2.63047	−10.1532	−10.1532	−2.63047	−2.63047	−10.1532	−9.81141
	std	3.818966	2.8E−12	1.91E−09	1.682133	2.210886	1.03E−05	0.090338
	Rank	7	1	2	5	6	3	4
F22	Best	−10.4029	−10.4029	−10.4029	−10.4029	−10.4029	−10.4029	−10.4029
	Average	−8.97137	−10.4029	−10.4029	−9.75463	−8.27887	−10.4029	−10.1364
	Median	−10.4029	−10.4029	−10.4029	−10.4029	−10.4029	−10.4029	−10.4029
	Worst	−2.7659	−10.4029	−10.4029	−2.75193	−5.08767	−10.4029	−5.07631
	std	2.945733	5.02E−15	3.82E−09	2.031123	2.668997	1.97E−07	1.191013
	Rank	6	1	2	5	7	3	4
F23	Best	−10.5364	−10.5364	−10.5364	−10.5364	−10.5364	−10.5364	−10.5364
	Average	−7.82085	−10.5364	−10.5364	−10.5364	−9.32552	−10.5364	−10.1522
	Median	−10.5364	−10.5364	−10.5364	−10.5364	−10.5364	−10.5364	−10.5364
	Worst	−2.42734	−10.5364	−10.5364	−10.5364	−3.83543	−10.536	−3.83543
	std	3.467724	2E−15	3.51E−09	1.58E−15	2.502342	8.46E−05	1.502943
	Rank	7	2	3	1	6	4	5
Average Rank		2.347826	2.73913	4.913043	4.608696	4.782609	3.608696	3.347826
Final ranking		1	2	7	5	6	4	3

than the comparison algorithm. ESNS outperforms other comparative techniques in the statistics of F1-F13 with Dim = 30 and the fixed dimensional functions F14-F23, which approves the significant dominance of ESNS in most functions compared to other techniques. Therefore, it can be concluded that the proposed ESNS technique exhibits the best performance compared to other algorithms.

4.3. Friedman's rank test results

Table 4 presents the statistical results obtained by Friedman tests [63]. The smaller the ranking value, the better the performance of the algorithm. From the results, we can get the ranks of five algorithms as follows: ESNS, SNS, MPA, EO, WHO, JS, and ARO. The highest ranking shows that ESNS is the best algorithm among the five algorithms.

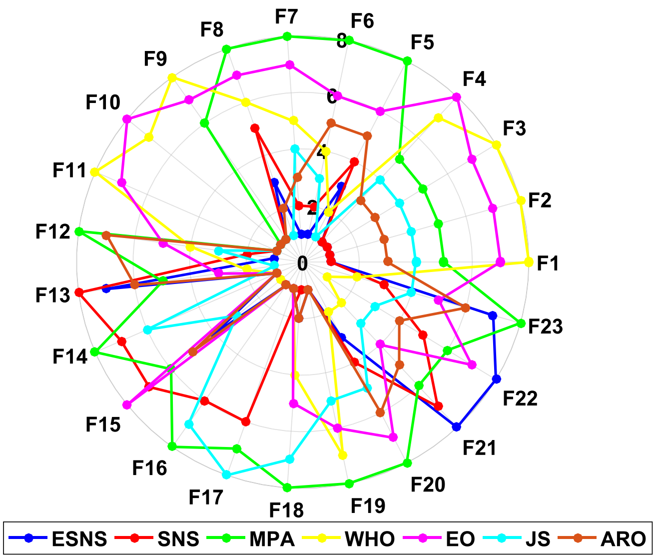

Fig. 3. Radar chart for ranks among all compared algorithms.

4.4. Result of engineering design problems

To assess the efficacy of the ESNS algorithm in addressing engineering optimization challenges, we conducted experiments on 13 real-world, non-convex, constrained optimization problems in chemical and mechanical engineering, sourced from CEC 2020. The violation of constraint functions' lower and upper limits was extracted from [64], and the obtained results were compared with those generated by alternative optimization algorithms, such as SNS, MPA, dung beetle optimizer (DBO) [65], and FOX [66]. Essential information about the benchmark functions used in the study is detailed in Tables 5 and 6. Given the presence of multiple inequality constraints in all these problems, any algorithm designed for their solution must incorporate a constraint-handling technique. Common approaches encompass repairing, decoding, preserving, and penalizing. In these case studies, we employed the firm penalty method to manage the constraints, with a population set at 200 for all 13 benchmarks and a maximum of 500 iterations for the case studies.

Table 7 showcases the statistical indexes' results for CEC 2020 non-convex optimization problems, comparing the performance of the ESNS algorithm with other optimization algorithms. The table also provides rankings for all thirteen case studies. The ranking order reveals the superior performance of the ESNS algorithm over the other compared algorithms across all 13 function problems. SNS and MPA demonstrate notable efficiency, securing the second and third optimal positions. This discussion leads to the conclusion that the ESNS algorithm proves to be an effective technique for finding optimal solutions to these types of problems.

The convergence characteristics of these algorithms for the specified functions are illustrated in Fig. 7. To further investigate and validate the performance of the proposed algorithm, Fig. 8 presents a boxplot of outcomes for each algorithm and objective function. Notably, Fig. 8 shows that the boxplots of the ESNS algorithm for most functions are narrow and among the smallest values, emphasizing its efficiency and effectiveness in comparison to the alternative algorithms.

4.5. The study cases

In this study, a series of thermal power systems with varying load levels are examined using the proposed ESNS algorithm. The systems under consideration include Case 1, which consists of an 11-unit system with a load level of 2,500 MW. Case 2 involves a 15-unit system with a load level of 2,630 MW. Furthermore, Case 3 encompasses a 40-unit system designed to accommodate a load level of 10,500 MW. Lastly, Case 4 presents a larger-scale 110-unit system capable of meeting a substantial load level of 15,000 MW. To investigate the performance of these systems, the proposed ESNS algorithm is applied. This algorithm is applied to enhance the operation and control of the thermal units in each case, aiming to achieve improved efficiency and reliability. In addition, a comparative study is shown by comparison the ESNS technique with other algorithms, namely artificial hummingbird algorithm (AHA) [67], RUN [68], GWO [69], GBO [70], and SNS. This comparison helps to evaluate the efficiency and superiority of the ESNS algorithm in terms of system performance, computational efficiency, and solution quality. Larger population sizes often lead to increased diversity within the population. This enhanced diversity can improve the algorithm's exploration capabilities by covering a broader search space. Consequently, the algorithm is more likely to find optimal solutions. However, an excessively large population might lead to slower convergence. The increased computational load from evaluating a larger population at each iteration can result in a longer time to reach convergence. Therefore, the population sizes are chosen for the medium population size, which is 500, for the four case studies to find the best solution and increase the convergence speed, simultaneously.

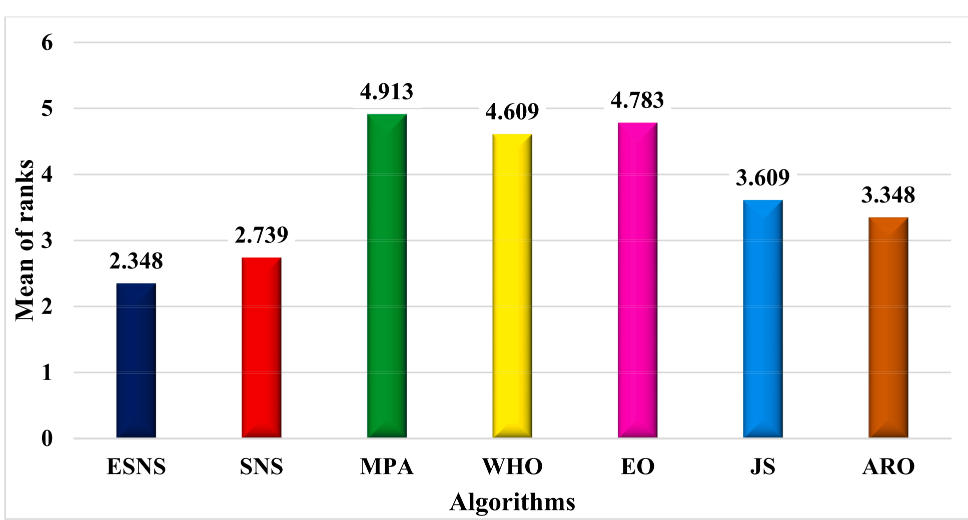

Fig. 4. Mean ranks obtained by tied rank test for 23 functions using various algorithms.

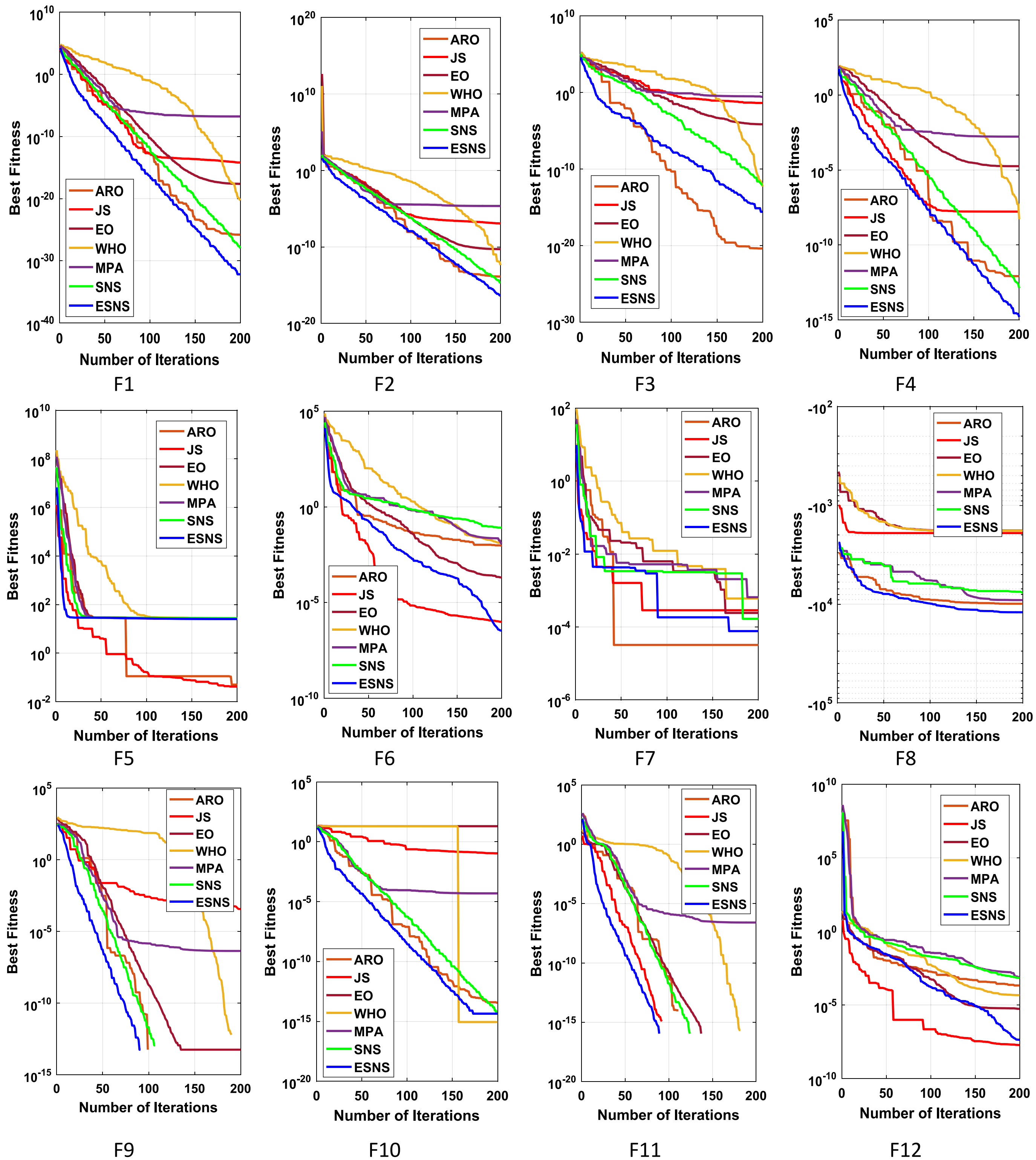

Fig. 5. The convergence curves of all techniques for twenty-three benchmark functions.

a) **Case 1 11 thermal units and the power demand (2500 MW).**

In this case, where there were 11 thermal units and a load demand of 2500 MW, the proposed ESNS algorithm stood out as the most effective in terms of minimizing fuel costs compared to other algorithms. System capacity and coefficient are taken from [71]. The ESNS technique provided the best solution values for fuel cost among the algorithms examined as shown in Table 8. Analyzing the power allocation for individual units (P1 to P11), the ESNS technique consistently allocated lower values to most units when compared to the other algorithms. This indicates that the ESNS algorithm achieved a more efficient distribution of power among the thermal units.

Specifically, the proposed ESNS algorithm achieved a fuel cost of $12,274.4 per hour, slightly outperforming the original SNS algorithm's

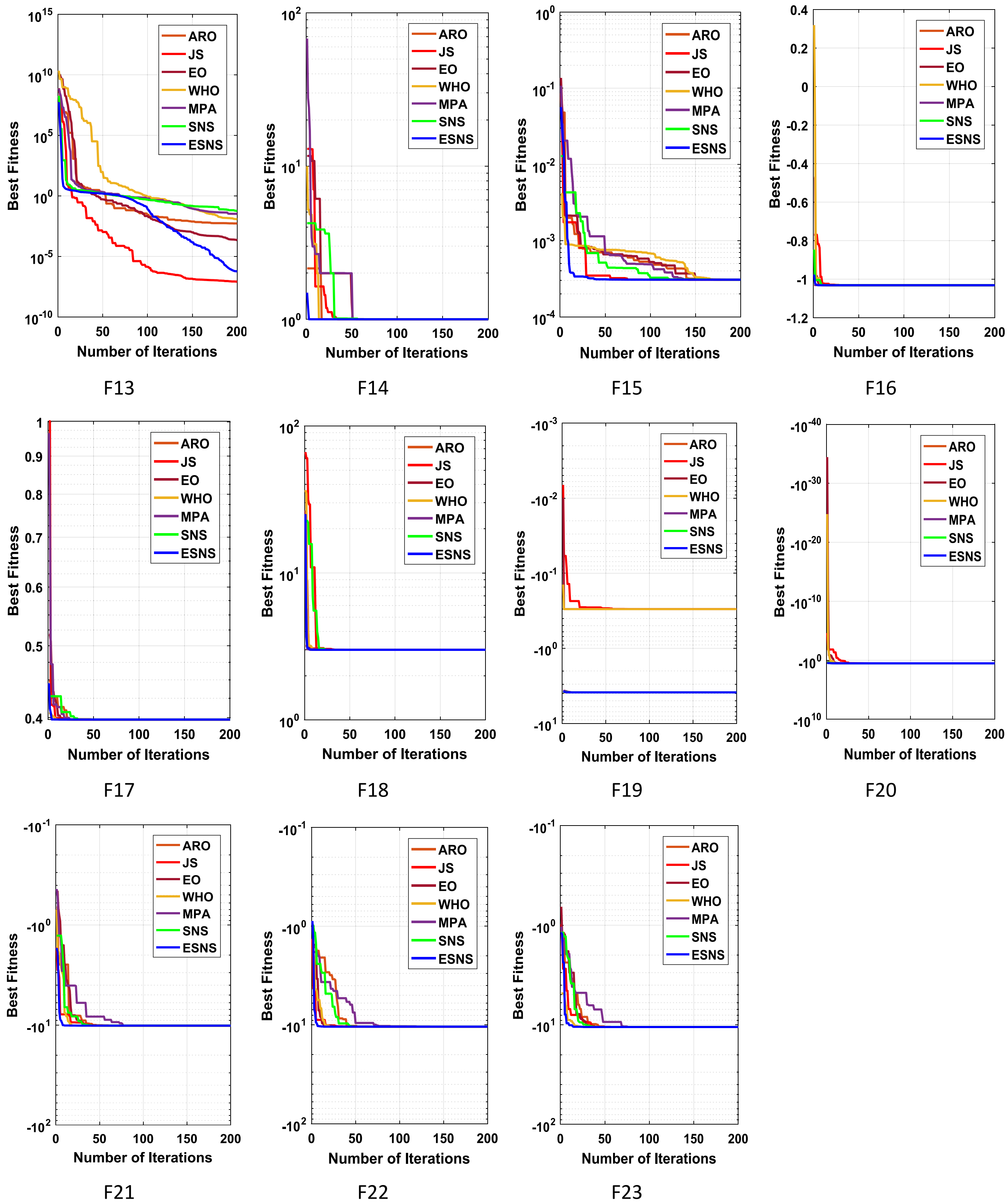

Fig. 5. (*continued*).

result of $12,274.44 per hour and equal to the GBO algorithm's result of $12,274.4 per hour. Furthermore, when compared to the RUN and GWO algorithms, the ESNS algorithm demonstrated superior performance, with fuel costs of $12,274.405 and $12,274.4124 per hour, respectively. These results highlight the effectiveness of the ESNS algorithm in minimizing fuel costs. Additionally, the ESNS algorithm showcased remarkable performance in constraint control. The violation (V) for the GBO algorithm and the proposed ESNS algorithm were the lowest value.

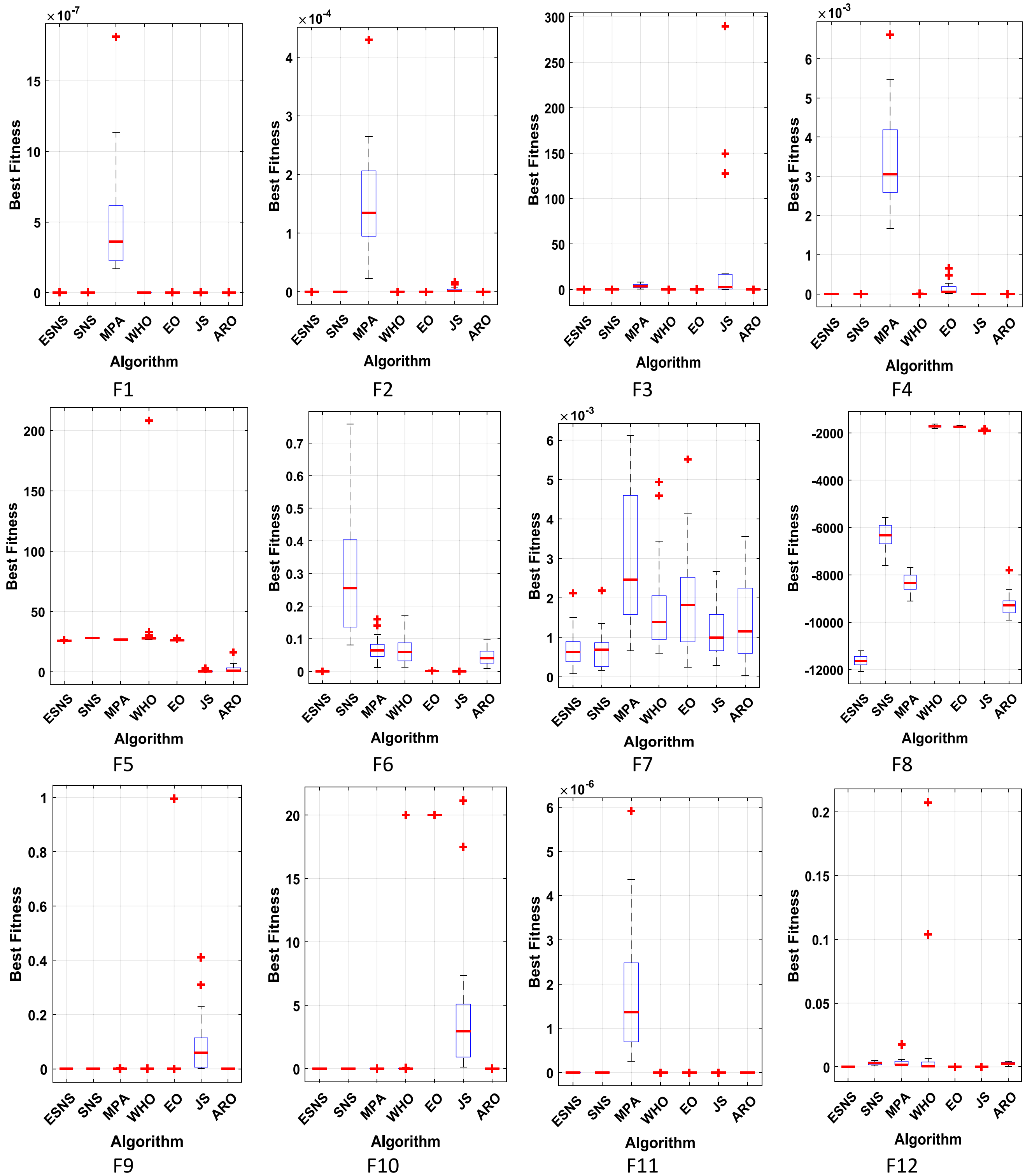

Fig. 6. Boxplots for all techniques for twenty-three benchmark functions.

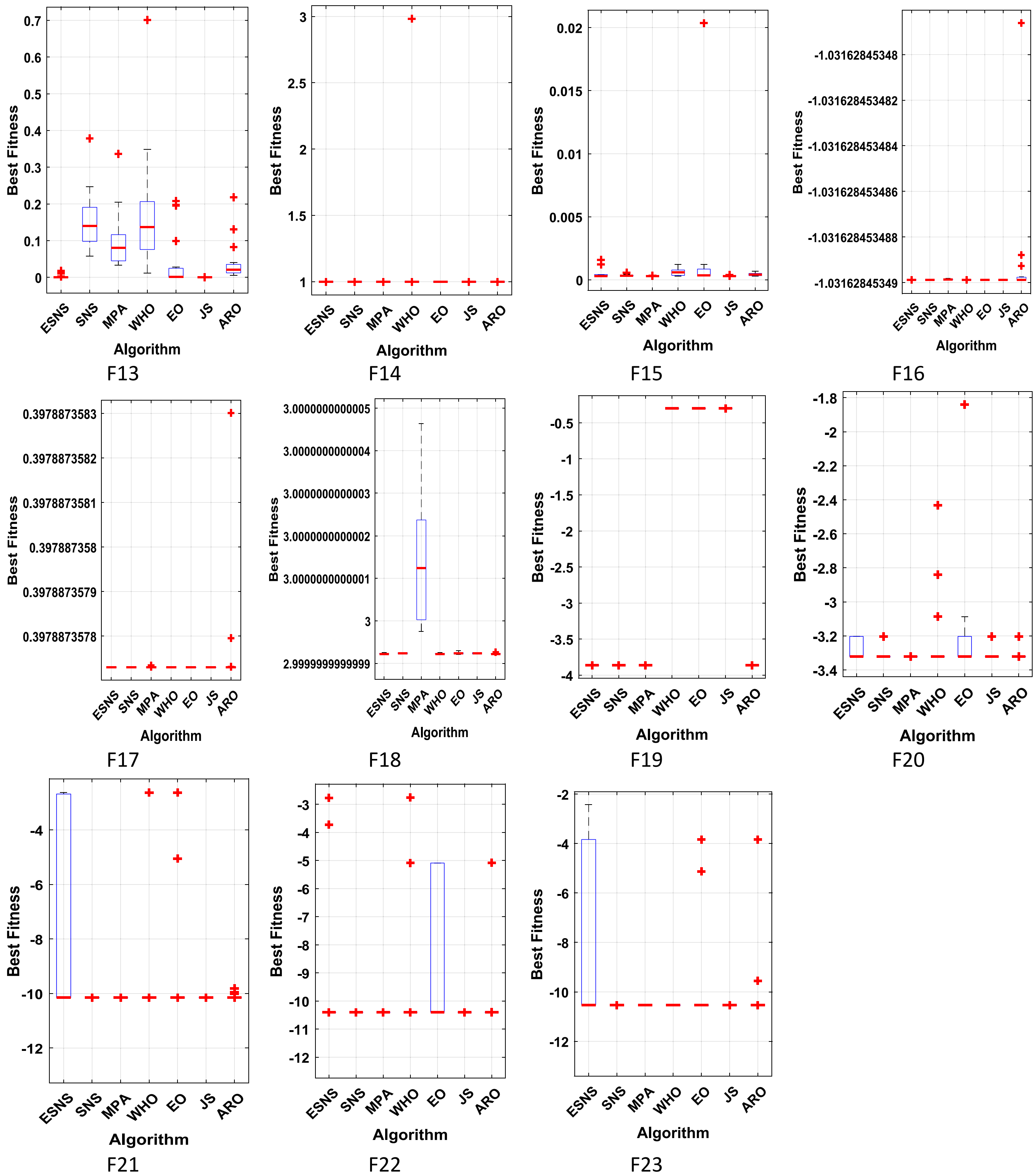

Fig. 6. (*continued*).

This indicates that the ESNS algorithm effectively managed and controlled the system's constraints, further enhancing its optimization capabilities. In summary, the ESNS algorithm excelled in minimizing fuel costs and optimizing power allocation in this case. Compared to the other algorithms, it provided the optimal fuel cost values, allocated power more efficiently, and effectively controlled the system's constraints.

Fig. 9 shows the fuel cost convergence curves of various optimization algorithms in the first case. Each technique's fuel cost values are plotted against the number of iterations, providing insights into the convergence behavior and optimization performance. The ESNS algorithm exhibits a consistently decreasing fuel cost as the iterations progress. The curve demonstrates a smooth convergence pattern, indicating the algorithm's ability to continuously improve the fuel cost solution. It showcases the

Table 3
Statistical results of the Wilcoxon rank-sum test.

ESNS vs	SNS		MPA		EO		WHO		JS		ARO	
Function	P	winner	P	winner	P	winner	P	winner	P	winner	P	winner
F1	6.796E−08	+	6.796E−08	+	6.796E−08	+	6.796E−08	+	6.796E−08	+	6.796E−08	+
F2	6.796E−08	+	6.796E−08	+	6.796E−08	+	6.796E−08	+	6.796E−08	+	6.796E−08	+
F3	6.796E−08	+	6.796E−08	+	6.796E−08	+	6.796E−08	+	6.796E−08	+	3.750E−04	–
F4	6.796E−08	+	6.796E−08	+	6.796E−08	+	6.796E−08	+	6.796E−08	+	6.796E−08	+
F5	6.796E−08	+	2.563E−07	+	4.680E−05	+	6.796E−08	+	6.796E−08	–	6.796E−08	–
F6	6.796E−08	+	6.796E−08	+	6.796E−08	+	6.796E−08	+	1.235E−07	+	6.796E−08	+
F7	9.892E−01	=	2.690E−06	+	3.382E−04	+	5.629E−04	+	1.794E−02	+	4.679E−02	+
F8	6.796E−08	+	6.796E−08	+	6.796E−08	+	6.796E−08	+	6.796E−08	+	6.796E−08	+
F9	NaN	=	8.007E−09	+	6.590E−09	+	3.500E−07	+	8.007E−09	+	NaN	=
F10	3.906E−04	+	8.007E−09	+	7.427E−10	+	3.988E−06	+	8.007E−09	+	8.007E−09	+
F11	NaN	=	8.007E−09	+	9.410E−03	+	3.421E−01	=	1.668E−04	+	NaN	=
F12	6.796E−08	+	6.796E−08	+	6.796E−08	+	6.796E−08	+	3.372E−02	+	6.796E−08	+
F13	6.796E−08	+	6.796E−08	+	9.278E−05	+	7.898E−08	+	7.764E−01	=	6.015E−07	+
F14	1.637E−01	=	6.828E−09	+	9.170E−05	+	7.749E−02	=	6.580E−07	+	1.536E−08	+
F15	1.075E−01	=	3.152E−02	–	9.032E−03	+	2.227E−02	+	4.407E−01	=	1.548E−02	+
F16	6.992E−04	+	1.117E−08	+	9.364E−03	+	2.084E−08	+	8.415E−02	=	1.783E−08	+
F17	1.334E−01	=	8.007E−09	+	7.797E−02	=	9.317E−01	=	3.998E−02	+	3.489E−07	+
F18	6.538E−01	=	5.296E−08	+	1.103E−09	+	1.103E−09	+	1.512E−08	+	6.912E−01	=
F19	5.146E−01	=	1.512E−08	+	7.420E−01	=	2.465E−02	–	2.074E−01	=	1.651E−08	+
F20	3.532E−02	+	5.970E−01	=	5.519E−01	=	7.154E−03	+	5.940E−01	=	4.397E−01	=
F21	5.940E−01	=	5.940E−01	=	1.251E−01	=	4.273E−01	=	8.963E−04	+	5.940E−01	=
F22	4.478E−01	=	8.963E−04	+	7.070E−01	=	6.449E−03	–	2.836E−01	=	8.963E−04	+
F23	6.796E−08	+	2.837E−01	=	6.796E−08	+	6.796E−08	+	6.796E−08	+	2.271E−01	=
WRST (+/=/−)	13/10/0		19/3/1		18/5/0		17/4/2		16/6/1		15/6/2	

Table 4
Friedman test for the seven algorithms.

Function	ESNS	SNS	MPA	EO	WHO	JS	ARO
F1	1	2	7	4.95	4	6	3.05
F2	1	2	7	4.7	4.3	6	3
F3	1.85	3.9	6.5	5.05	3.1	6.45	1.15
F4	1	2	7	6	4.45	4.5	3.05
F5	3.15	6.75	4.85	4.1	6.15	1.2	1.8
F6	1	6.9	5.35	3	5.2	2	4.55
F7	2.75	2.5	5.75	5	4.6	3.75	3.65
F8	1	4	2.95	6.45	6.55	5	2.05
F9	2.075	2.075	5.9	4.325	4.6	6.95	2.075
F10	1.35	1.85	4.65	6.85	4.15	6.05	3.1
F11	3.05	3.05	7	3.925	3.25	4.675	3.05
F12	1.25	5.65	5.6	3	4.8	1.75	5.95
F13	1.7	6.2	5.1	3.55	6.05	1.45	3.95
F14	2.125	2.575	6.825	3.775	2.75	4.375	5.575
F15	3.5	4.05	1.65	4.95	5.35	3.05	5.45
F16	2.05	3.4	6.55	2.95	4.475	2.55	6.025
F17	3.075	3.075	6.75	3.075	3.075	3.075	5.875
F18	2.925	3.775	7	4.125	2.975	4.075	3.125
F19	1.525	1.525	4	5.5	5.5	7	2.95
F20	3.825	4.05	3.95	3.675	2.5	4.4	5.6
F21	4.175	2.325	4.6	3.65	2.05	5.3	5.9
F22	3	2.275	5.15	4.45	2.575	4.6	5.95
F23	4.025	2.65	5.4	3.55	1.725	4.55	6.1
Mean ranks	2.278261	3.416304	5.501087	4.373913	4.094565	4.293478	4.042391

effectiveness of the ESNS algorithm in finding an optimal solution for the given case study. In comparison, the GBO algorithm's convergence curve shows a slower rate of improvement in fuel cost. Although it gradually decreases over iterations, it appears to converge at a higher fuel cost value than the ESNS algorithm.

The RUN algorithm's convergence curve displays a fluctuating pattern, with occasional dips and rises in fuel cost values. This suggests that the optimization process may encounter challenges in reaching a stable and optimal solution for the given case study. The original SNS algorithm's convergence curve shows an initial rapid decrease in fuel cost, but it eventually plateaus without further significant improvement. This suggests that the algorithm may have encountered convergence limitations or reached a suboptimal solution for the case study. The GWO algorithm's convergence curve shows a relatively slow convergence rate. It exhibits a gradual decrease in fuel cost but does not reach a significantly low value compared to the other techniques. This shows that the GWO may struggle to find an optimal solution within the given iterations. Overall, the figure of fuel cost convergence curves provides a visual representation of how different techniques perform in optimizing the fuel cost for Case Study 1. It highlights the superior convergence and optimization capabilities of the ESNS algorithm, while also showcasing the varying degrees of performance and convergence exhibited by the other techniques.

Fig. 10 presents boxplots comparing the performance of various optimization algorithms in the first case. The boxplots provide a visual representation of the distribution and statistical characteristics of the fuel cost results obtained from each technique. Each boxplot represents the fuel cost values generated by a specific optimization technique. The

Table 5
Problem definition for the engineering benchmark cases as in the CEC 2020 real-world non-convex constrained optimization problems [64].

serial no.	Functions	case study	Decision variables	constraints	global optima
1	RC8	Process synthesis problem	2	2	2.00E + 00
2	RC12	Process synthesis problem	7	9	2.92E + 00
3	RC13	Process design Problem	5	3	2.69E + 04
4	RC15	Weight Minimization of a Speed Reducer	7	11	2.99E + 03
5	RC17	Tension/ compression spring design (case 1)	3	3	1.27E−02
6	RC18	Pressure vessel design	4	4	5.89E + 03
7	RC19	Welded beam design	4	5	1.67E + 00
8	RC20	Three-bar truss design problem	2	3	2.64E + 02
9	RC21	Multiple disk clutch brake design problem	5	7	2.35E−01
10	RC28	Rolling element bearing	10	9	1.46E + 04
11	RC29	Gas Transmission Compressor Design (GTCD)	4	1	2.96E + 06
12	RC31	Gear train design Problem	4	1	0.00E + 00
13	RC32	Himmelblau's Function	5	6	−3.07E + 04

Table 6
Bounds of the engineering benchmark cases [64].

Functions	Lower and upper bounds
RC8	$0 \le x_1 \le 1{:}6$; x_2 ε {01}
RC12	$0 \le x_2$; x_3; $x_1 \le 100$; x_7; x_6; x_5; x_4 ε {01}
RC13	$27 \le x_3$; $x1$; $x_2 \le 45$; x_4 ε {78, 79, …. 102}; x_5 ε {33, 34, …. 45}
RC15	$0{:}7 \le x_2 \le 0{:}8$; $17 \le x_3 \le 28$; $2{:}6 \le x_1 \le 3{:}6$ $5 \le x_7 \le 5{:}5$; $7{:}3 \le x_5$; $x_4 \le 8{:}3$; $2{:}9 \le x_6 \le 3{:}9$
RC17	$0{:}05 \le x_1 \le 2{:}00$; $0{:}25 \le x_2 \le 1{:}30$; $2{:}00 \le x_3 \le 15{:}0$
RC18	$10 \le x4$; $x_3 \le 200$; $1 \le x_2$; $x_1 \le 99$ (integer variables)
RC19	$0{:}1 \le x_3$; $x_2 \le 10$; $0{:}1 \le x_4 \le 2$; $0{:}125 \le x_1 \le 2$
RC20	$0 \le x_1$; $x_2 \le 1$
RC21	$60 \le x_1 \le 80$; $90 \le x_2 \le 110$; $1 \le x_3 \le 3$; $0 \le x_4 \le 1000$; $2 \le x_5 \le 9$
RC28	x_1 ε {125 150}; x_2 ε {10.5 31}; x_3 ε {4.51 50.49}; x_4 ε {0.515 0.6}; x_5 ε {0.515 0.6} x_6 ε {0.4 0.5}; x_7 ε{0.6 0.7}; x_8 ε {0.3 0.4}; x_9 ε{0.02 1}; x_{10} ε {0.6 0.85}
RC29	$20 \le x_1 \le 50$; $1 \le x_2 \le 10$; $20 \le x_3 \le 50$; $0{:}1 \le x_4 \le 60$
RC31	$12 \le x_2$; x_3; x_4; $x_1 \le 60$
RC32	$78 \le x_1 \le 102$; $33 \le x_2 \le 45$; $27 \le x_3$, x_4, $x_5 \le 45$;

box itself depicts the interquartile range (IQR), showing the middle 50 % of the data. The line inside the box represents the median fuel cost, indicating the central tendency of the results. The whiskers extend from the box to the minimum and maximum fuel cost values, excluding outliers. Any data points outside the whiskers are represented as individual points, denoting potential outliers.

The boxplots allow for a comparative analysis of the different techniques. The height and spread of the boxes provide insights into the variability and dispersion of the fuel cost results. A taller and wider box indicates greater variability, while a narrower box suggests more consistent results.

By examining the boxplots, we can observe that The ESNS technique exhibits a relatively narrow box, indicating less variability and consistent performance. The median fuel cost is positioned at a lower value, suggesting that the ESNS algorithm consistently achieves better fuel cost solutions. The GBO technique displays a wider box, suggesting higher variability in the fuel cost results. The median fuel cost is positioned at a slightly higher value compared to the ESNS algorithm, indicating a less optimal performance. The RUN technique shows a box that indicates higher variability and poorer fuel cost solutions compared to both ESNS and GBO techniques. The SNS technique exhibits a wide box with a relatively high median fuel cost value. This indicates significant variability and suboptimal fuel cost results compared to the other techniques. The GWO technique's boxplot shows a wide box, indicating high variability and inconsistent performance. The median fuel cost value is positioned relatively high, suggesting suboptimal solutions compared to the ESNS algorithm. In summary, the boxplots in Fig. 10 provide a visual comparison of the fuel cost results obtained from different optimization techniques in Case Study 1. The ESNS algorithm demonstrates superior performance with lower variability and better fuel cost solutions compared to the other algorithms, while the remaining techniques exhibit higher variability and suboptimal results.

Table 9 shows the statistical results for the first case, comparing different optimization algorithms based on their fuel cost values. The table includes information such as the best, worst, median, average, and standard deviation (std.) of the fuel cost results. The ESNS algorithm achieved the best fuel cost value of 12,274.4. It also had the same value for the worst, median, and average fuel costs, indicating consistent performance. The standard deviation was very low at 0.000823, suggesting minimal variability in the fuel cost results. In summary, Table 9 provides statistical measures for the fuel cost results obtained from different optimization algorithms in Case 1. The ESNS algorithm achieved the best and most consistent fuel cost values, with the lowest standard deviation. The other algorithms displayed varying levels of performance and variability, with the BWO algorithm exhibiting the highest standard deviation and potentially less optimal fuel cost solutions.

b) **Case 2 15 units and the power demand 2630 MW.**

In Case 2, which involves a system consisting of 15 generating units and a load demand of 2630 MW, the ESNS algorithm was utilized to optimize the fuel cost. This system contains 15 units, its capacity and coefficient are taken from [4]. Some generating units in this system have no POZ, while one generator has two POZs and others have three ones. The coefficients of the system to attain power losses are given in [4]. Table 10 provides the optimal solution values obtained for the fuel cost by comparing the ESNS algorithm with other optimization techniques. The ESNS algorithm produced the optimum solution for the fuel cost, resulting in a value of $32,693.08 per hour. Comparatively, the SNS algorithm achieved a fuel cost of $32,724.42 per hour, the GBO algorithm yielded $32,717.26 per hour, the RUN algorithm obtained $32,700.58 per hour, and the GWO algorithm achieved $32,740.74 per hour. Analyzing the power output for individual units (P1 to P15), the ESNS algorithm allocated power values that were generally close to those of the other algorithms. However, some slight differences can be observed in specific units. For instance, in P1, the ESNS algorithm allocated 454.9995 MW, while other algorithms allocated either 455 MW or slightly lower values. Similar variations can be seen in other units as well. The ESNS algorithm successfully controlled the system's constraints, as indicated by the violation (V) value of approximately 1.65E−07 MW, which was the lowest among all the algorithms. This highlights the algorithm's effectiveness in managing and satisfying the constraints imposed by the system. In summary, the ESNS algorithm demonstrated superior performance in minimizing fuel cost in this case. It outperformed other optimization techniques, achieving the lowest fuel cost value. The ESNS algorithm also showcased efficient constraint control, resulting in a negligible violation compared to the other algorithms.

Fig. 11 presents the convergence curves of five optimization

Table 7
Results of statistical indexes for the engineering benchmark cases.

Functions	Index	ESNS	SNS	MPA	DBO	FOX
RC8	Min	2	2	2	2	2
	Average	2	2	2	2	2
	Median	2	2	2	2	2
	Max	2	2	2	2	2
	std	2.34E−16	2.34E−16	8.27E−12	2.44E−16	7.1E−08
	Rank	1	1	4	1	5
RC12	Min	2.924831	2.924831	2.924848	2.924831	2.924872
	Average	2.924831	2.924832	3.210192	3.378957	2.946508
	Median	2.924831	2.924832	2.947026	3.081732	2.925031
	Max	2.924831	2.924834	4.20646	4.074353	3.082564
	std	1.41E−07	8.76E−07	0.526884	0.481632	0.047529
	Rank	1	2	4	5	3
RC13	Min	26887.42	26887.42	26887.42	26887.42	26887.42
	Average	26887.42	26887.42	26887.42	26887.42	27135.01
	Median	26887.42	26887.42	26887.42	26887.42	26887.42
	Max	26887.42	26887.42	26887.42	26887.42	28368.22
	std	0	0	9.24E−10	1.12E−11	473.4105
	Rank	2	2	4	1	5
RC15	Min	2994.424	2994.424	2994.434	2994.424	2995.595
	Average	2994.424	5E + 14	2994.464	6E + 14	6.5E + 14
	Median	2994.424	5E + 14	2994.451	1E + 15	1E + 15
	Max	2994.424	1E + 15	2994.536	1E + 15	1E + 15
	std	1.15E−08	5.27E + 14	0.034797	5.03E + 14	4.89E + 14
	Rank	1	3	2	4	5
RC17	Min	0.012665	0.012666	0.012665	0.012666	0.012677
	Average	0.012667	0.012672	0.012665	0.012742	5E + 13
	Median	0.012666	0.012671	0.012665	0.012719	0.012781
	Max	0.012676	0.012681	0.012665	0.012928	1E + 15
	std	3.24E−06	4.33E−06	5.11E−08	7.56E−05	2.24E + 14
	Rank	2	3	1	4	5
RC18	Min	6247.676	6247.673	6247.673	6247.673	6359.528
	Average	6273.322	6247.695	6247.675	6544.502	39927.73
	Median	6247.708	6247.691	6247.673	6382.985	15046.06
	Max	6405.048	6247.767	6247.682	7319.001	239304.1
	std	50.69662	0.0276	0.002945	400.6724	65645.18
	Rank	3	2	1	4	5
RC19	Min	1.670218	1.670218	1.670218	1.670218	1.67593
	Average	1.670218	1.670218	1.67022	1.700254	1.756922
	Median	1.670218	1.670218	1.670219	1.670218	1.722726
	Max	1.670218	1.670218	1.670226	1.816712	1.994586
	std	9.35E−12	1.42E−10	2.67E−06	0.055884	0.080852
	Rank	1	2	3	4	5
RC20	Min	263.8958	263.8958	263.8958	263.8958	263.8958
	Average	263.8958	263.8959	263.8958	263.8959	263.8959
	Median	263.8958	263.8959	263.8958	263.8959	263.8959
	Max	263.8959	263.8959	263.8958	263.8961	263.8962
	std	8.12E−06	1.09E−05	2.57E−08	4.76E−05	7.87E−05
	Rank	2	3	1	4	5
RC21	Min	0.235242	0.235242	0.235242	0.235242	0.235242
	Average	0.235242	0.235242	0.235242	0.235242	0.235243
	Median	0.235242	0.235242	0.235242	0.235242	0.235243
	Max	0.235242	0.235242	0.235242	0.235242	0.235243
	std	2.93E−17	2.93E−17	1.44E−10	1.14E−16	9.23E−08
	Rank	1	1	4	3	5
RC28	Min	5599.448	5599.448	5599.448	5599.448	5599.448
	Average	5599.448	5599.448	5599.448	5599.448	5599.448
	Median	5599.448	5599.448	5599.448	5599.448	5599.448
	Max	5599.448	5599.448	5599.448	5599.448	5599.448
	std	0	0	0	0	0
	Rank	1	1	1	1	1
RC29	Min	2,964,896	2,964,896	2,964,895	2,964,895	2,989,723
	Average	2,964,896	2,964,897	2,964,895	3,011,451	3,086,914
	Median	2,964,896	2,964,897	2,964,895	2,964,897	3,096,913
	Max	2,964,897	2,964,899	2,964,895	3,147,942	3,104,538
	std	0.485489	0.974712	0.000697	74628.94	29668.78
	Rank	2	3	1	4	5
RC31	Min	3.89E−23	1.17E−16	4.23E−23	0	3.38E−19
	Average	3.22E−20	1.28E−13	7.45E−21	0	4.3E−17
	Median	1.46E−20	5.09E−14	1.58E−21	0	6.21E−18
	Max	1.49E−19	4.93E−13	3.22E−20	0	3.28E−16
	std	4.76E−20	1.95E−13	1.13E−20	0	8.09E−17
	Rank	3	5	2	1	4
RC32	Min	−30665.5	−30665.5	−30665.5	−30665.5	−30665.5
	Average	−30665.5	−30665.5	−30665.5	−30665.5	−30648.6

(continued on next page)

Table 7 (*continued*)

Functions	Index	ESNS	SNS	MPA	DBO	FOX
	Median	−30665.5	−30665.5	−30665.5	−30665.5	−30665.5
	Max	−30665.5	−30665.5	−30665.5	−30665.5	−30514.8
	std	2.97E−12	6.75E−12	0.000401	3.73E−12	41.5896
	Rank	2	2	4	1	5
Average Rank		1.692308	2.307692	2.461538	2.846154	4.461538
Final ranking		1	2	3	4	5

algorithms in the second case. The convergence curves provide insights into the performance and progress of each technique in minimizing the fuel cost over successive iterations. The x-axis of the figure denotes the number of iterations, while the y-axis signifies the fuel cost value. Each line on the graph corresponds to a specific optimization technique, showcasing how the fuel cost evolves. In the case of ESNS, its convergence curve illustrates the trend of decreasing fuel cost as the algorithm progresses. Initially, the fuel cost may be relatively high, but as the iterations advance, the curve steadily descends toward lower values. This indicates the continuous improvement and optimization of the fuel cost by the ESNS algorithm. By comparing the convergence curves of different techniques, we can gain insights into their relative performance. If the ESNS curve consistently exhibits the steepest decline and reaches the lowest fuel cost value, it indicates that the ESNS algorithm is highly effective in minimizing the fuel cost.

Fig. 12 illustrates boxplots comparing the performance of studied optimization algorithms in the second case. The boxplots provide statistical summaries and visual representations of the fuel cost results obtained from each technique. By examining the boxplots of different techniques, we can compare their performance in terms of fuel cost. the boxplot for ESNS demonstrates a lower median fuel cost value and a narrower spread, it suggests that the ESNS technique consistently achieves better results in decreasing the fuel cost compared to other techniques. Additionally, the presence of outliers in the boxplots can provide insights into the variability and potential suboptimal solutions produced by each technique. A smaller number of outliers in the ESNS boxplot indicates a more stable and reliable performance in minimizing fuel cost.

Table 11 presents the optimal solution values of fuel cost for the 15-unit system in Case Study 2. The table compares the performance of various optimization algorithms in terms of their fuel cost results. Among the listed algorithms, the ESNS algorithm achieved the best fuel cost value of 32693.08, indicating its effectiveness in minimizing the cost of fuel consumption. The ESNS algorithm also demonstrated the smallest standard deviation (1.639649) among all the algorithms, suggesting a high level of consistency in its performance. Comparing ESNS with other algorithms, it outperformed the SNS, GBO, RUN, and GWO techniques in terms of the best fuel cost value obtained. The ESNS algorithm also exhibited a lower median and mean fuel cost compared to other algorithms, indicating its robustness in achieving favorable results. It's worth noting that several other algorithms were tested in this case study, but their results are not comparable due to missing information in the table, such as worst, median, mean, and standard deviation values. Overall, Table 11 highlights the superior performance of the ESNS algorithm in minimizing the fuel cost for the 15-unit system. Its ability to consistently achieve lower fuel costs, along with its relatively low standard deviation, signifies its effectiveness in optimizing the operation of the power system.

c) **Case 3 40 generating units and the power demand (MW).**

In this case, a comprehensive power generation system involving of 40 generating units is studied, and tests are conducted under two different scenarios. The system data and the generation bounds and the coefficients of fuel cost used in this case study are obtained from [15]. The obtained generation schedules are shown in Table 12. Analyzing Table 12, it is evident that the proposed ESNS algorithm outperforms other techniques, including SNS, RUN, GBO, and GWO algorithms. The results obtained from ESNS are consistently better than those achieved by other algorithms. To further examine the convergence behaviors, Fig. 13 illustrates the fuel cost convergence curves for the ESNS, SNS, RUN, GBO, and GWO algorithms. This figure demonstrates the superior performance of the ESNS algorithm in solving the ELD problem, thereby validating the effectiveness of the proposed technique. In summary, the results from Case 3 highlight the effectiveness of the ESNS algorithm in minimizing fuel costs for the forty-unit system. Its superior performance, as evident in both the obtained results and convergence behavior, reinforces the viability and reliability of the proposed ESNS technique for optimizing power generation systems.

Fig. 14 presents the boxplots of studied algorithms used in the third case for the 40-unit power generation system. The boxplots provide a visual representation of the statistical distribution of the fuel cost values obtained from each algorithm. Among the techniques compared, the ESNS algorithm's boxplot stands out, indicating its superior performance in minimizing fuel costs. The boxplot shows a smaller interquartile range and lower median value compared to the other techniques, suggesting more consistent and better results. In contrast, the boxplots of the other techniques demonstrate larger interquartile ranges and higher median values, indicating a wider spread of fuel cost values and potentially less optimal solutions. Overall, the boxplot of the ESNS algorithm in Fig. 14 provides compelling evidence of its effectiveness in achieving lower fuel costs compared to the other techniques tested in Case Study 3.

Table 13 presents the statistical results for this case, comparing various algorithms used in the optimization of a 40-unit power generation system. The table includes measures such as the best solution, average, median, worst solution, and standard deviation of the fuel cost values obtained by each algorithm. Among the algorithms evaluated, the ESNS algorithm demonstrates competitive performance. It achieves a best fuel cost value of 121,415.6 and a median value of 121,713.7, indicating its ability to find cost-effective solutions. The average fuel cost obtained by ESNS is 121,742.2, which suggests consistent performance across multiple iterations. The worst solution found by ESNS is 122,155.2, indicating its capability to handle challenging scenarios. The standard deviation of 206.7005 signifies the algorithm's stability and limited variability in results. Comparatively, other algorithms such as SNS, GBO, RUN, and GWO also produce reasonably competitive results, although they exhibit slightly higher fuel costs and larger standard deviations than ESNS. Additionally, Table 13 includes results from alternative techniques such as EBWO, BWO, SCSO, SOA, FOX, ISMA, SMA, HHO, JS, TSA, PSO, PPSO, SSA, MPA, MGMPA, and HSSA. These algorithms show varying levels of performance in terms of fuel cost optimization. Overall, the statistical results in Table 13 affirm the effectiveness of the ESNS algorithm in achieving lower fuel costs compared to other techniques, showcasing its potential as a robust optimization approach for the forty-unit power system.

d) **Case 4 110 generating units and the power demand (15,000 MW).**

In Case 4, we consider a large-scale power generation system comprising 110 thermal units with a load demand of 15,000 MW. To tackle the complexity of this system, the maximum number of iterations

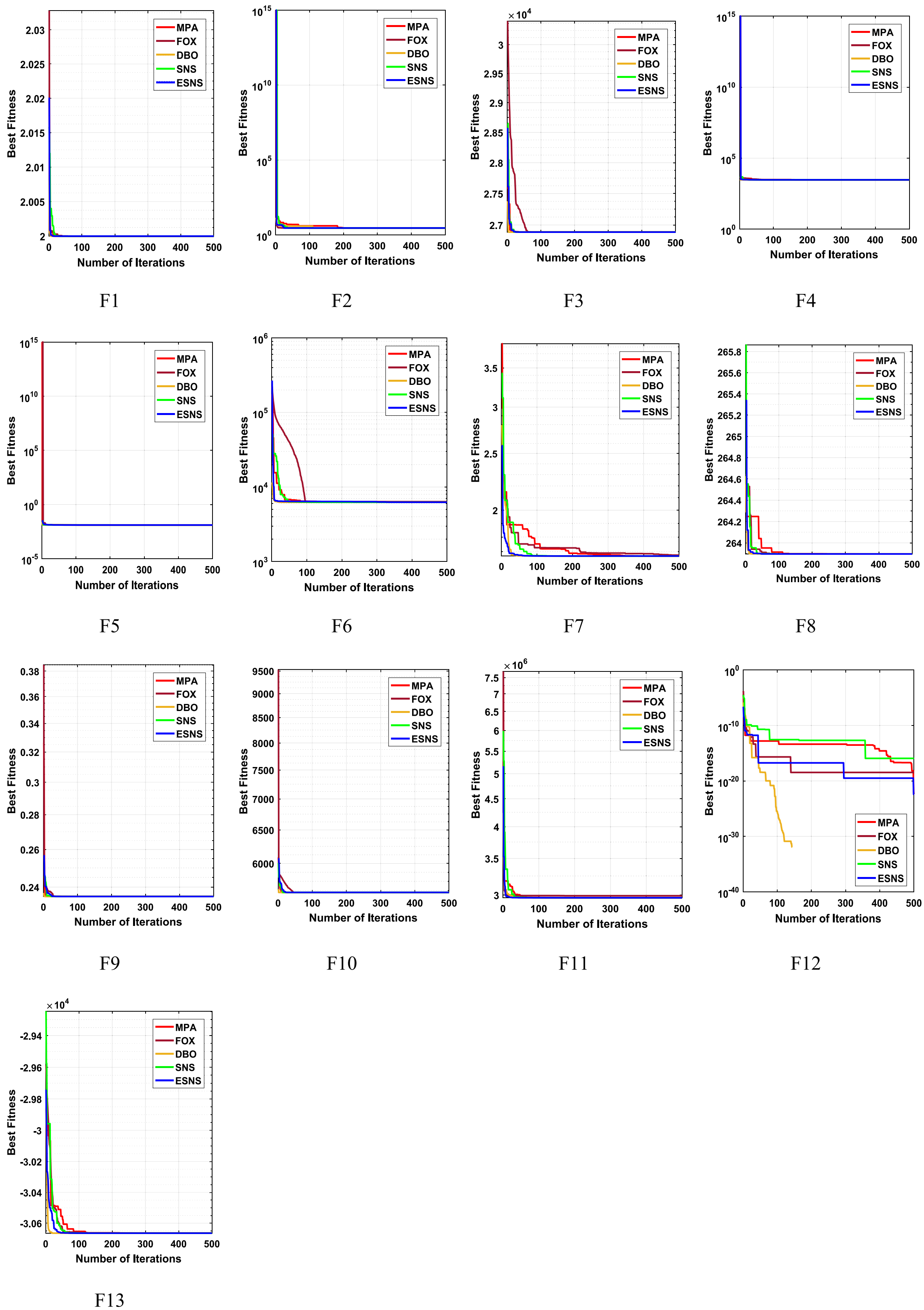

Fig. 7. The convergence curves for all techniques and benchmark functions.

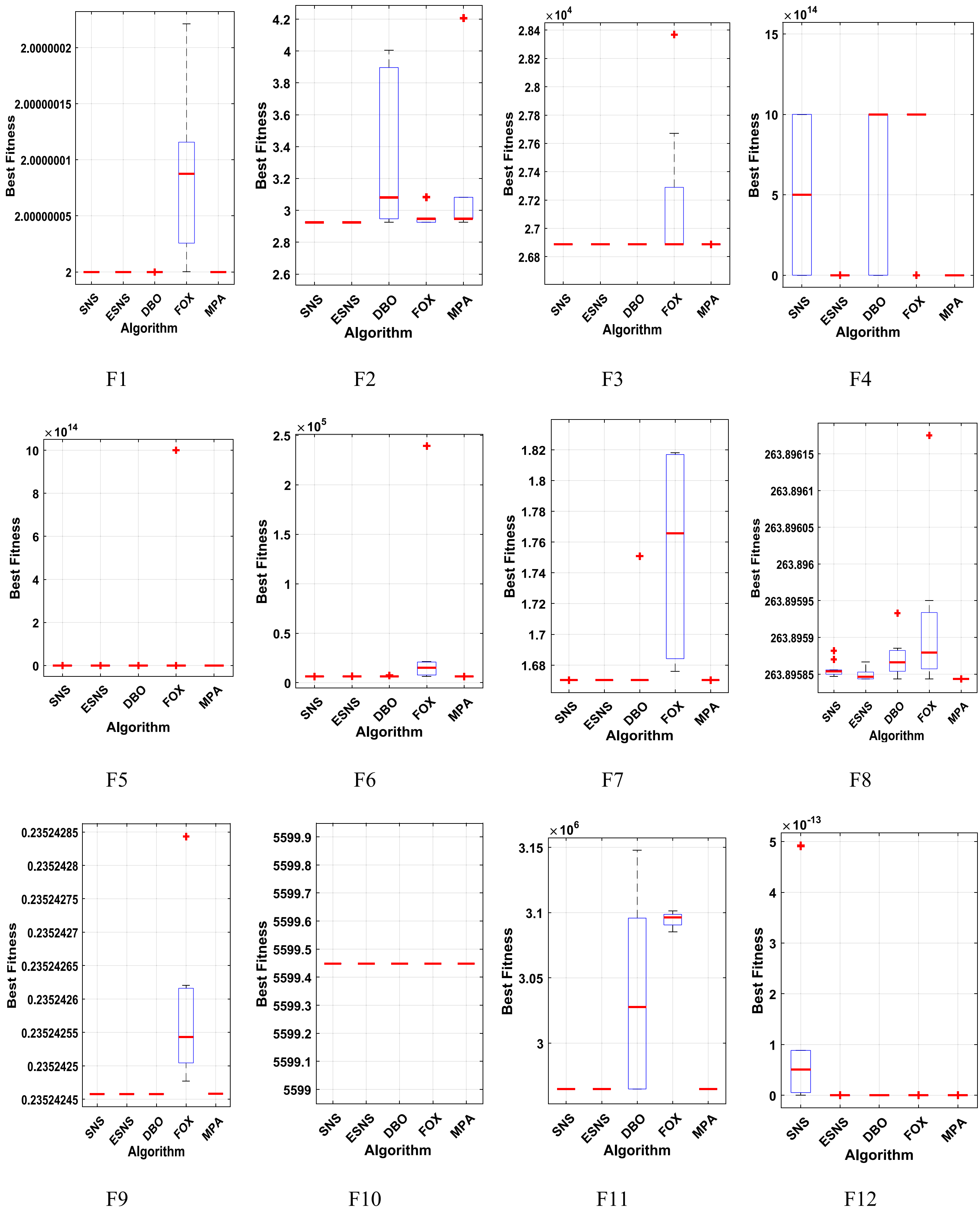

Fig. 8. Boxplots for all techniques and benchmark functions.

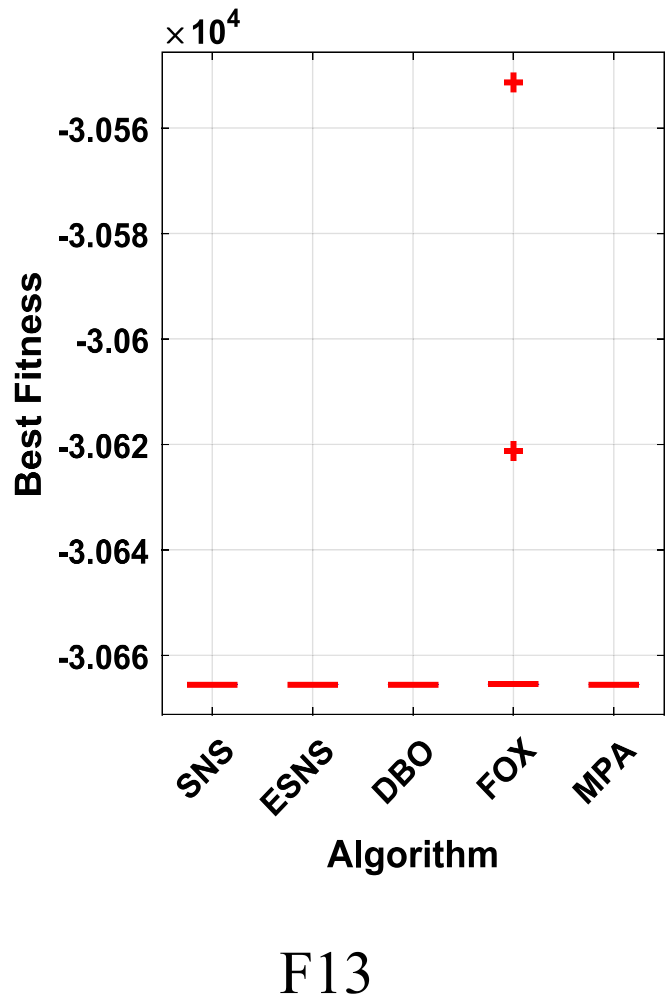

Fig. 8. (*continued*).

Table 8
The best fuel cost values for the 11-unit system.

Method	ESNS	SNS	GBO	RUN	GWO
P1 (MW)	57.1211	55.86796	56.9012	57.027	57.4219
P2 (MW)	40.5027	40.63254	40.4154	40.289	40.9249
P3(MW)	57.8806	57.98805	57.7161	57.614	57.962
P4 (MW)	277.622	277.4494	278.024	276.91	278.334
P5 (MW)	187.1	185.4905	187.015	187.4	185.891
P6 (MW)	249.104	248.4461	249.394	249.16	249.536
P7 (MW)	177.018	175.0647	176.983	177.21	176.873
P8 (MW)	380.135	379.5498	379.946	380.53	379.035
P9 (MW)	341.638	343.5276	341.498	340.56	341.241
P10 (MW)	378.829	382.4858	378.335	379.1	377.408
P11 (MW)	353.048	353.497	353.771	354.19	355.373
V(MW)	1.7E−05	6.10E−04	3E−06	6.4E−05	3E−05
Fuel Cost($/h)	12274.4	12274.44	12274.4	12274.41	12274.41

for the ESNS, SNS, RUN, GBO, and GWO algorithms has been increased to 1500. This extended iteration limit aims to improve the overall performance of these algorithms and improve their ability to find optimal solutions in such a large-scale setting. Table 14 presents the optimal solution values obtained by these techniques for the 110-unit system. The table showcases the effectiveness of these algorithms in minimizing fuel cost, which is a vital objective in ELD problems. The specific values of the best solution for each algorithm are listed in the table. These values represent the optimum allocation of power generation among the thermal units that results in the lowest fuel cost for the given system and load demand. The algorithms are compared based on their ability to find near-optimal solutions and achieve lower fuel costs. By examining Table 14, we can analyze the performance of the ESNS algorithm in comparison to the other algorithms for the 110-unit power system. The algorithm's best solution value reflects the lowest fuel cost achieved by ESNS among all the tested algorithms. The results presented in Table 14 validate the capability of the ESNS algorithm to effectively optimize the power generation schedule and minimize fuel costs in a large-scale system. These findings emphasize the potential of the ESNS algorithm for addressing complex ELD problems and its value in practical power system operation and planning.

The ESNS algorithm's convergence curve depicts the trend of the fuel

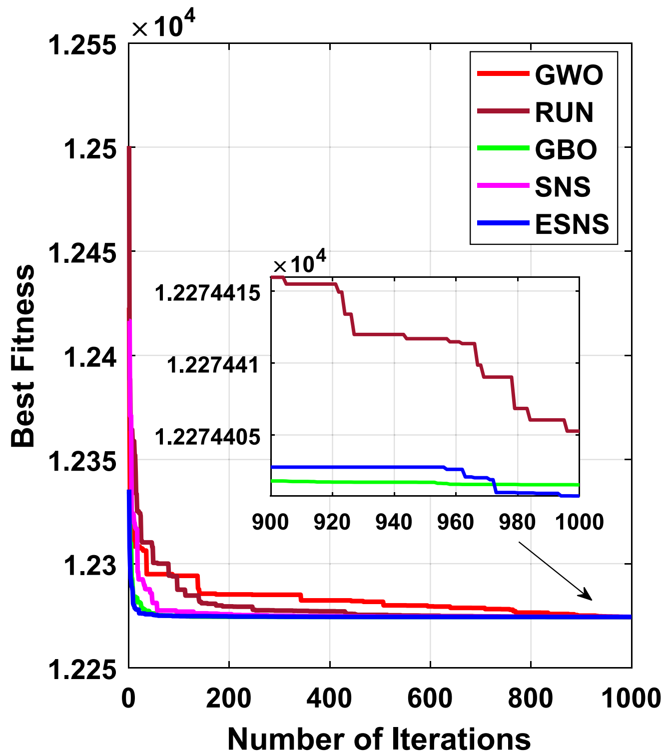

Fig. 9. The convergence curves of the proposed ESNS and other recent algorithms for case 1.

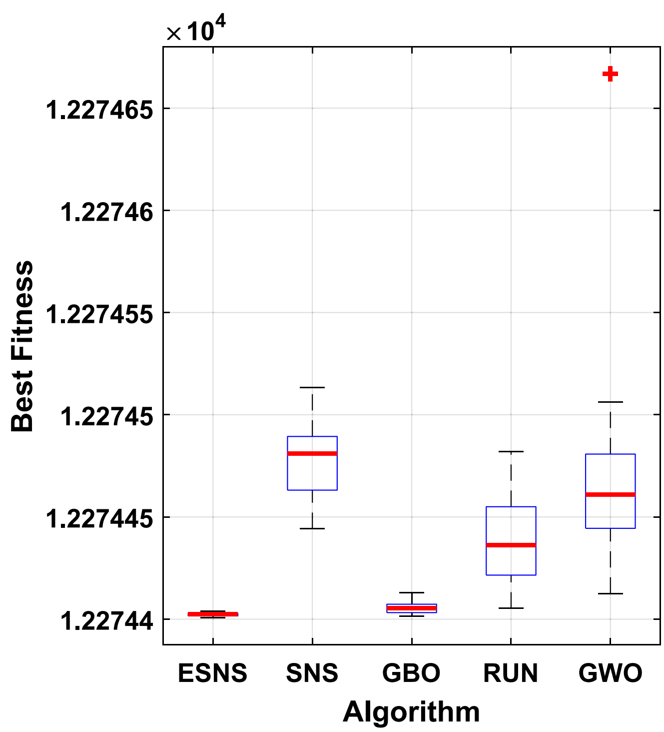

Fig. 10. boxplots of different algorithms for case 1.

cost values obtained by the algorithm over the course of the iterations. By observing the curve, we can analyze the algorithm's ability to iteratively improve the fuel cost and converge toward an optimal or near-optimal solution. A steeper descent in the curve indicates faster progress towards lower fuel costs, while a gradual slope suggests a slower

Table 9
Statistical results of the proposed ESNS and other algorithms for Case 1.

Method	Best	Average	Median	Worst	Std.
ESNS	12274.4	12274.4	12274.4	12274.4	0.000823
SNS	12274.44	12274.48	12274.48	12274.51	0.019719
GBO	12274.4	12274.41	12274.41	12274.41	0.002919
RUN	12274.41	12274.44	12274.44	12274.48	0.024704
GWO	12274.41	12274.47	12274.46	12274.67	0.051635
EBWO [72]	12274.46	12274.55	12274.54	12274.7	0.065663
BWO [72]	12278.83	12285.32	12285.54	12292.9	3.633401
FOX [72]	12274.57	12275.69	12275.48	12278.27	0.869111
ISMA [15]	12274.4	12274.41	12274.41	12274.4	0.001423
SMA [15]	12274.4	12274.41	12274.41	12274.41	0.001163
HHO [15]	12274.4	12274.45	12274.41	12274.42	0.0096
JS [15]	12274.4	12274.4	12274.4	12274.4	0.000652
TSA [15]	12276.19	12285.53	12277.43	12278.44	2.732958
PSO [15]	12274.4	12274.56	12274.42	12274.44	0.04804

Table 10
The optimal solution values for the fuel cost of the fifteen−unit system.

Method	ESNS	SNS	GBO	RUN	GWO
P1 (MW)	454.9995	455	454.9998	455	452.9496
P2 (MW)	379.9973	379.8621	379.9995	379.9748	378.1478
P3(MW)	129.9999	127.8087	129.9998	130	129.8193
P4 (MW)	130	129.0656	130	130	130
P5 (MW)	169.9662	164.1047	152.4773	169.9998	164.2171
P6 (MW)	459.998	459.4698	459.9973	459.9864	458.7296
P7 (MW)	429.9975	429.5793	430	429.9992	428.9978
P8 (MW)	83.34011	77.60301	60.07531	60.02533	67.02907
P9 (MW)	46.8508	92.92797	88.13783	101.355	83.29008
P10 (MW)	159.472	133.5842	159.2346	127.3228	134.238
P11 (MW)	79.99452	75.76096	80	79.99605	78.06923
P12 (MW)	79.99942	79.34187	79.99992	79.78253	73.3213
P13 (MW)	25.04299	25	25.01132	25.33732	25.1814
P14 (MW)	15.00001	15.98873	15.03286	15.49778	26.74054
P15 (MW)	15.0085	15	15.37101	15.02823	28.58303
Ploss (MW)	29.6667	30.1262	30.3366	29.3055	29.3104
V(MW)	1.65E−07	0.029308	9.72E−11	0.000188	0.003361
Fuel Cost($/h)	32693.08	32724.42	32717.26	32700.58	32740.74

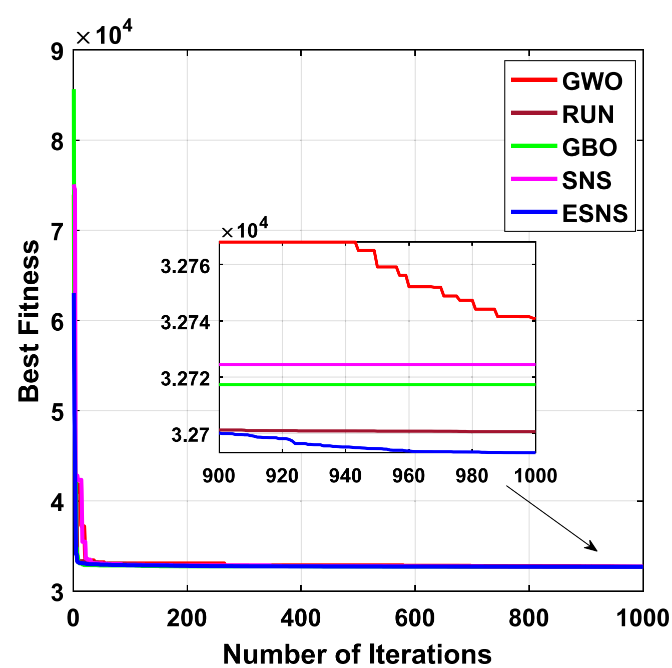

Fig. 11. The convergence curves of the proposed ESNS and other recent algorithms for case 2.

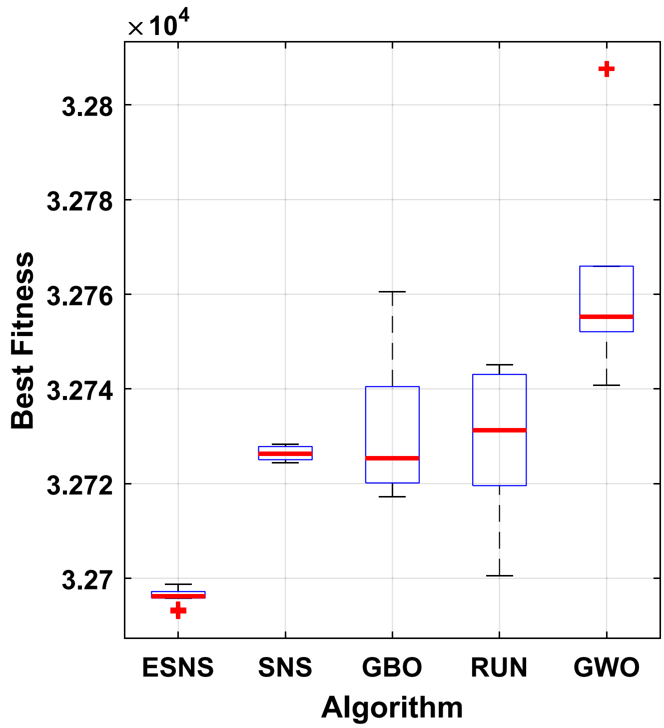

Fig. 12. Boxplots of different algorithms for case 2.

convergence rate. Fig. 15 also includes the fuel cost convergence curves of other techniques, enabling a comparison of their performance with ESNS. The curves of different techniques allow us to assess their convergence behavior, rate of improvement, and potential for achieving lower fuel costs. By evaluating the position and trend of the ESNS algorithm's fuel cost convergence curve in comparison to the other techniques, we can gain a deeper understanding of its performance and its potential for addressing complex ELD problems in practical power systems.

In Case Study 4, Fig. 16 presents boxplots representing the fuel cost distribution of different techniques, including the ESNS algorithm. By examining the ESNS algorithm's boxplot in Fig. 16, we can assess its fuel cost distribution and compare it with the distributions of other techniques. The relative position of the ESNS boxplot to the others provides insights into its competitiveness in terms of fuel cost performance. Additionally, the spread of the ESNS boxplot indicates the algorithm's variability in obtaining different fuel cost values. Comparing the boxplots of different techniques in Case Study 4 helps us evaluate the performance, robustness, and effectiveness of the ESNS algorithm in addressing the economic load dispatch problem for the large-scale 110-unit power generation system. It provides a visual representation of how the algorithm's fuel cost results compare to other state-of-the-art techniques and allows for a comprehensive assessment of its optimization capabilities.

Table 15 provides the statistical results for Case 4, presenting the fuel cost performance of various algorithms, including the ESNS algorithm, applied to the 110-unit power generation system with a load demand of 15,000 MW. The table includes several key statistical measures that offer insights into the fuel cost distribution achieved by each algorithm. Analyzing the results in Table 15 for the ESNS algorithm, we can observe its performance compared to other techniques. The ESNS algorithm achieved a best fuel cost value of 200,266.5, a worst value of 202,925.5, a median value of 203,669.1, and an average value of 204,908. The standard deviation for the ESNS algorithm is 1,669.812, indicating a moderate level of variability in the fuel cost results. By comparing the results of the ESNS algorithm with other techniques in Table 15, we can assess its competitiveness and efficiency in minimizing the fuel cost for

Table 11
The optimal solution values for the 15-unit system.

Method	Best	Average	Median	Worst	STD
ESNS	32693.08	32696.05	32696.18	32698.71	1.639649
SNS	32724.42	32726.41	32726.27	32728.27	1.381541
GBO	32717.26	32731.07	32725.32	32760.49	14.24217
RUN	32700.58	32730.47	32731.32	32745.06	12.96173
GWO	32740.74	32759.39	32755.24	32807.62	13.28598
HHO [39]	32,863.05	–	–	33153.54	153.2478
HHO-AβHC [39]	32,694.73	–	–	32698.74	2.2276
SCA-βHC [73]	32,761.56	–	–	32,799.42	15.7
SCA [73]	33,236.41	–	–	34,690.21	161
CLCS-CLM [74]	32,704.45	–	–	32704.45	–
CPSO [75]	32835.00	–	–	33021.00	–
CS [74]	32704.45	–	–	32704.75	–
CS-CLM [74]	32704.45	–	–	32704.45	–
GAPSO [76]	32724.00	–	–	32984.00	–
HBF [77]	32784.50	–	–	32976.81	–
HS [78]	32813.34	–	–	32910.65	–
IHS [78]	32830.34	–	–	32925.26	–
IPSO [75]	32709.00	–	–	32784.50	–
PSO [75]	32858.00	–	–	33039.00	–
PVHS [78]	32780.00	–	–	32892.46	–
SOH-PSO [79]	32751.39	–	–	32878.00	–
EO [80]	32701.18	32701.51	–	32701.31	–
ABC [81]	32787.836	–	–	32791.5366	–
FA [82]	32704.5	33,175	–	32856.1	–
MPSO-GA [83]	32,702	32755.19	–	32701.31	–
EO-SCA [84]	32700.51	32701.05	–	32702.74	–
PSOSIF [85]	32,706.88	32,709.92	–	32,707.79	3.04
GAAPI [86]	32,732.95	32,756.01	–	32,735.06	–
FA [82]	32,704.45	33,175.00	–	32,856.10	–
EPSO [87]	32,704.83	32,762.01	–	32,725.37	–
IAEDP [88]	32,698.20	32,823.78	–	32,750.22	29.2989
EMA [89]	32,704.45	32,704.45	–	32,704.45	–
GABC [90]	32,706.66	32706.81	–	32,706.69	0.035838
TLBO [91]	32,697.22	32,697.22	–	32,697.22	0
Jaya [92]	32712.6458	32822.9993	–	32743.4613	47.0256
Jaya-M [92]	32707.0312	32743.6808	–	32714.4386	12.0972
Jaya-SM [92]	32706.983	32728.2292	–	32709.0463	8.7817
Jaya-SML [92]	32706.3578	32707.2925	–	32706.6764	2.3244
TS [93]	32917.87	33245.54	–	33066.76	66.82

(*continued on next page*)

Table 11 (*continued*)

Method	Best	Average	Median	Worst	STD
DSPSO-TS [93]	32715.06	32730.39	–	32724.63	8.4
BF-NM [77]	32784.5024	–	–	32976.81	85.77
CSO [35]	32709.36	32722.55	–	32712.49	4.56
CCSO [35]	32706.64	32706.64	–	32706.64	0.0007

the large-scale 110-unit power generation system. The lower the fuel cost values and standard deviation, the more effective the algorithm is in achieving cost optimization and maintaining consistency in its results. These statistical results provide valuable insights into the performance of the ESNS algorithm and enable a comprehensive evaluation of its effectiveness in addressing the economic load dispatch problem in a complex and demanding system.

4.6. A. Wilcoxon's rank test results

The Wilcoxon rank-sum test results are presented in Table 16, providing statistical insights into the comparisons between the ESNS algorithm and other algorithms (SNS, GBO, RUN, and GWO) across different test cases. For Case 1, ESNS is significantly better than SNS, GBO, RUN, and GWO, with p-values of 6.7956E−08, 9.2780E−05, 6.7956E−08, and 6.7956E−08, respectively. ESNS emerges as the winner in all comparisons. In Case 2, ESNS is again significantly better than SNS, GBO, RUN, and GWO, with p-values of 6.1266E−08, 5.2497E−08, 5.4047E−08, and 5.4600E−08, respectively. Similar to Case 1, ESNS dominates in all comparisons. For Case 3, ESNS is statistically equivalent (indicated by '=') to SNS, but significantly better than GBO, RUN, and GWO. The p-values for these comparisons are 5.6517E−02, 7.8980E−08, 3.4156E−07, and 3.4156E−07, respectively. In Case 4, ESNS is significantly better than SNS and GBO with p-values of 6.1529E−08 and 3.0691E−06, respectively. However, its performance is not significantly different from RUN (p-value: 3.5859E−04), and it is statistically equivalent to GWO (p-value: 2.1841E−01). These Wilcoxon rank-sum test results shed light on the comparative performance of the ESNS algorithm against the other algorithms, providing valuable insights into their relative strengths across different test cases.

4.7. Friedman's rank test results

The results of Friedman's rank test were analyzed for the performance of seven different algorithms across multiple test cases. Table 17 displays the ranks assigned to each algorithm in each case, with algorithms ESNS, SNS, GBO, RUN, and GWO. In Case 1, ESNS obtained the lowest rank of 1.05, while SNS and GWO received ranks of 4.65 and 4.05, respectively. GBO and RUN fell in between with ranks of 2.05 and 3.2. For Case 2, ESNS secured the lowest rank of 1, while SNS, GBO, RUN, and GWO followed with ranks of 2.95, 3.05, 3.05, and 4.95. In Case 3, GBO achieved the highest rank of 4.7, while ESNS, SNS, RUN, and GWO received ranks of 1.75, 1.35, 3.85, and 3.35. Case 4 presents ESNS and GBO gaining ranks of 1.8 and 3.8, respectively. SNS and RUN received ranks of 4.85 and 3.05, while GWO achieved the lowest rank of 1.5. The mean ranks across all cases indicate that ESNS had the lowest average rank of 1.4, suggesting it performed well on average. SNS followed with a mean rank of 3.45, GBO with 3.4, RUN with 3.2875, and GWO with 3.4625.

Furthermore, Fig. 17 visually represents the mean ranks obtained from Friedman's rank test for four different cases using the various algorithms. This visualization provides a clear comparison of the algorithms' performances across the cases, helping to identify any significant

Table 12
The optimal solution values of the 40-unit system.

Method	ESNS	SNS	GBO	RUN	GWO
P1 (MW)	111.8716	110.8046	114	113.7667	111.318
P2 (MW)	111.7829	110.9735	114	113.8196	113.29
P3(MW)	97.40065	97.40021	120	98.35404	112.0964
P4 (MW)	179.7338	179.7333	179.7331	179.7409	180.2536
P5 (MW)	88.87531	91.96816	96.99999	95.52452	90.17506
P6 (MW)	140	139.9998	140	125.161	140
P7 (MW)	259.6019	259.6037	299.9997	264.8556	300
P8 (MW)	284.6011	284.6029	290.6229	286.1997	292.6191
P9 (MW)	284.6005	284.6078	284.6131	287.6533	287.0849
P10 (MW)	130.0002	204.7999	279.5997	130.0021	130.8928
P11 (MW)	168.8001	94.00099	94.00005	168.782	94.30928
P12 (MW)	168.7998	168.8001	168.7998	168.8236	168.9356
P13 (MW)	214.7599	214.7604	214.7598	214.7431	125
P14 (MW)	394.2795	304.5184	304.5196	304.5213	304.4093
P15 (MW)	394.2794	394.2794	394.2794	304.5446	484.0966
P16 (MW)	304.5196	394.2796	125.0005	394.2737	304.982
P17 (MW)	489.2794	489.2792	489.2794	489.2933	490.1055
P18 (MW)	489.2799	489.2797	489.2794	489.283	489.7544
P19 (MW)	511.2796	511.2794	511.2794	511.2879	511.8928
P20 (MW)	511.2796	511.2802	511.2794	511.2876	511.699
P21 (MW)	523.2797	523.2793	523.2794	523.294	524.8197
P22 (MW)	523.2795	523.28	523.2794	523.2941	523.5176
P23 (MW)	523.2795	523.2793	523.2794	523.3055	524.4795
P24 (MW)	523.28	523.2823	523.2794	523.2948	524.2936
P25 (MW)	523.2801	523.2794	523.2794	523.2825	523.2721
P26 (MW)	523.28	523.2807	523.2794	523.3032	524.3899
P27 (MW)	10.00022	10.0006	10	10.0056	11.7591
P28 (MW)	10.0001	10.00055	10	10.00229	11.69244
P29 (MW)	10.00017	10.00037	10	10.00172	10.13242
P30 (MW)	89.57694	88.33986	97	93.88226	93.40904
P31 (MW)	189.9999	190	190	189.9987	189.9209
P32 (MW)	190	189.9996	190	189.9997	189.9654
P33 (MW)	190	189.9998	190	189.9444	190
P34 (MW)	164.8036	164.8059	199.9993	165.7906	177.3923
P35 (MW)	164.8223	164.8143	200	199.9195	185.8648
P36 (MW)	164.8137	164.8213	200	199.8445	199.6596
P37 (MW)	110	110	109.9999	93.65193	108.1539

(*continued on next page*)

Table 12 (*continued*)

Method	ESNS	SNS	GBO	RUN	GWO
P38 (MW)	109.9999	109.9992	110	95.33708	110
P39 (MW)	109.9999	109.9997	110	109.9358	109.8542
P40 (MW)	511.2794	511.2793	511.2794	549.9939	511.9656
V(MW)	3.37E−04	7.24E−03	4.22E−09	3.41E−04	12.5439
Fuel Cost ($/h)	121415.6	121465.7	122103.7	121912.6	121951.3

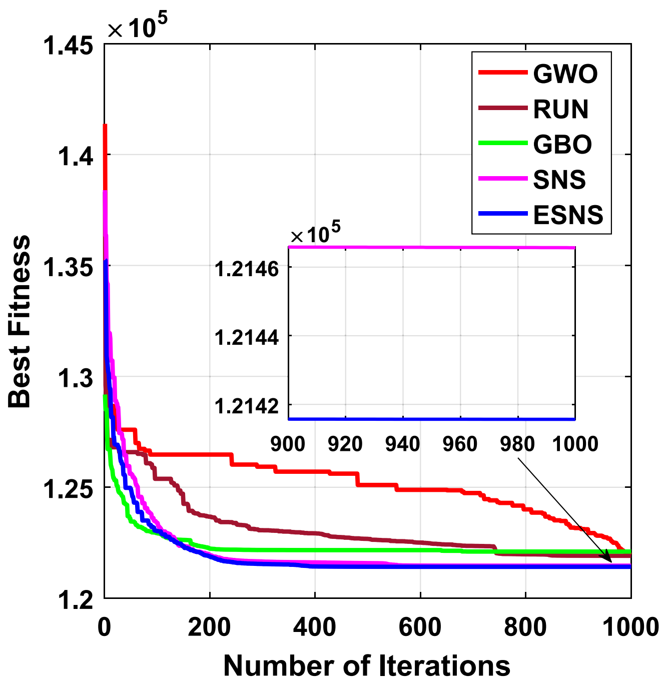

Fig. 13. The convergence curves of the proposed ESNS and other recent algorithms for case 3.

differences in their ranks.

4.8. Computational time

This subsection provides insights into the computational efficiency of their proposed method in comparison to other algorithms. This information is crucial for assessing the practicality of implementing the proposed method in real-world scenarios. The average CPU time serves as a metric to quantify the computational efficiency of the algorithms. This metric indicates the average amount of time the algorithms require to complete their computations, measured in terms of CPU processing time. To ensure statistical significance, the authors conducted 20 runs of each algorithm and then calculated the average CPU time across these runs. The results of the computational time analysis are presented in Table 18. This table displays the average CPU time for different algorithms (ESNS, SNS, GBO, RUN, GWO) on various test systems with different numbers of units (11-unit, 15-unit, 40-unit, 110-unit). The average CPU time values are provided in the table for each combination of algorithm and test system.

Fig. 18 visualize the average CPU time data for different algorithms on different test Each algorithm is represented by a distinct bar, and each test system is associated with a specific data point on the graph. The x-axis represents the test systems with different numbers of units, while the y-axis represents the average CPU time. Each bar's height

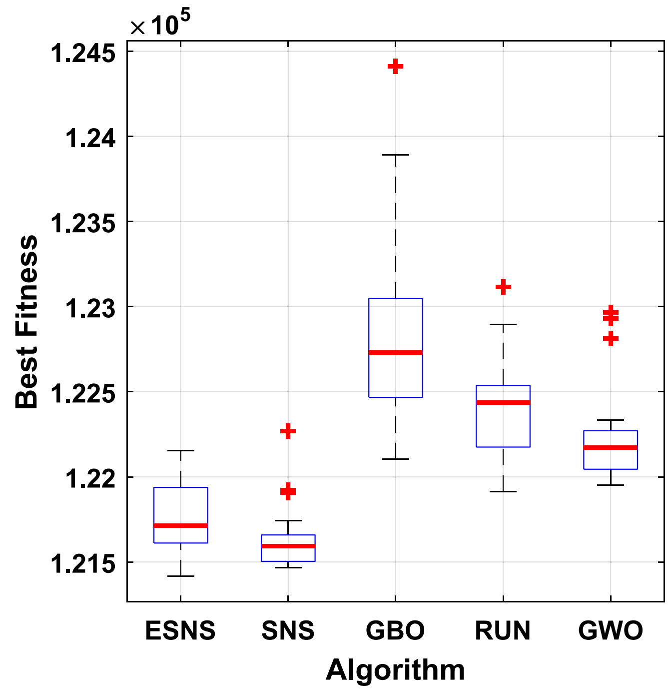

Fig. 14. Boxplots of the proposed ESNS and other recent algorithms for case 3.

Table 13
the Statistical results of the fuel cost using several optimization algorithms for Case 3.

Method	Best	Average	Median	Worst	Std.
ESNS	121415.6	121742.2	121713.7	122155.2	206.7005
SNS	121465.7	121640.8	121593.2	122267.9	194.8689
GBO	122103.7	122859.7	122729.4	124411.4	577.6911
RUN	121912.6	122413.3	122,437	123114.8	310.3578
GWO	121951.3	122254.1	122171.9	122965.9	299.9711
EBWO [72]	121600.9	122012.6	121991.8	122180.9	163.4211
BWO [72]	122875.8	123398.6	123395.8	123858.9	240.7044
SCSO [72]	123633.3	125219.7	125210.6	128464.7	1092.271
SOA [72]	125704.4	127019.5	127074.1	128066.9	667.1643
FOX [72]	123745.7	125954.3	126112.2	129811.1	1391.512
ISMA [15]	121546.89	121702.82	121726.95	121859.73	164.1745
SMA [15]	121621.68	121770.54	121781.88	121994.65	153.4794
HHO [15]	122439.24	122966.90	122974.36	123801.25	364.4271
JS [15]	122577.7	123181.8	123,331	123,413	246.9075
TSA [15]	125385.34	125628.15	125368.53	126380.35	661.7595
PSO [15]	121627.99	121893.32	121892.71	122077.55	151.4660
PSO [12]	126487.71	129613.92	–	130049.36	2363.06
PPSO [12]	125503.09	127886.04	–	129631.35	1033.37
SSA [12]	123565.75	125408.20	–	127442.23	905.64
MPA [12]	123180.98	124750.53	–	126614.40	927.37
MGMPA [12]	122634.69	123939.11	–	125523.19	755.10
HSSA [44]	121960.27	122239.53	–	–	–

indicates the average CPU time for the corresponding algorithm on a specific test system. This graph presents quickly compare the computational efficiency of the algorithms across different test systems. It becomes evident which algorithms perform better in terms of computational time under varying system sizes. It demonstrates the proposed ESNS's ability to consistently attain optimal solutions across various test cases, even though it demands longer CPU times than its algorithmic counterparts. The long CPU times also give valuable insights into the complexity of the problems being tackled. The proposed ESNS algorithm tries to find the optimal solutions and these extended processing times serve as a testament to the intricacies and challenges inherent in the optimization problem.

Table 14
The optimal solution values of the 110-unit system.

Method	ESNS	SNS	GBO	RUN	GWO
P1 (MW)	4.396819	2.4	12	4.304815	7.307189
P2 (MW)	4.075666	2.4	12	2.4	3.758552
P3(MW)	4.444906	4.840947	2.4	2.40087	11.27568
P4 (MW)	6.866255	2.4	2.4	2.426355	4.644202
P5 (MW)	4.357672	2.615427	2.400002	2.44357	3.009219
P6 (MW)	4.087036	4	4	4.001954	4.391267
P7 (MW)	4	12.42562	4	6.378918	4.803595
P8 (MW)	4.176884	20	4	4.645362	9.265834
P9 (MW)	4.737287	4	4	4	17.26776
P10 (MW)	68.7276	32.44262	76	15.20251	17.58897
P11 (MW)	38.27302	76	76	15.2	22.12444
P12 (MW)	17.46777	76	15.2	50.44753	34.07952
P13 (MW)	72.50605	26.95375	76	16.67627	50.16429
P14 (MW)	33.63005	64.03202	100	70.57824	48.20954
P15 (MW)	34.26905	25	25.0006	25.02376	33.80927
P16 (MW)	30.27341	98.7397	25	80.38302	32.55901
P17 (MW)	128.5514	60.0134	155	150.6839	153.7419
P18 (MW)	154.9941	140.0132	155	86.13621	146.9209
P19 (MW)	150.2492	87.9442	54.3	155	152.2013
P20 (MW)	154.0879	94.0478	54.30001	120.176	146.636
P21 (MW)	68.9	78.16154	189.5873	71.50172	70.71392
P22 (MW)	69.69063	86.44323	68.90039	75.17649	71.68416
P23 (MW)	70.96428	133.2475	68.90001	68.9	69.73388
P24 (MW)	329.239	309.2896	350	350	338.2159
P25 (MW)	389.4244	396.1684	400	399.9382	400
P26 (MW)	394.3661	398.2161	400	400	398.6603
P27 (MW)	491.1771	463.978	500	500	489.3208
P28 (MW)	488.298	500	500	498.5611	464.5661
P29 (MW)	175.4392	158.8764	200	200	196.5196
P30 (MW)	87.73448	52.44466	100	32.16522	31.92832
P31 (MW)	14.58612	36.54978	10	10	10.15611
P32 (MW)	19.0881	18.31002	5	6.663588	7.676521
P33 (MW)	42.07327	72.17863	20	49.64464	45.26159
P34 (MW)	250	250	250	106.1709	246.9746
P35 (MW)	329.3661	360	360	360	353.8889
P36 (MW)	400	400	400	400	377.9885
P37 (MW)	25.53483	25.58462	39.99994	25.29133	19.33672
P38 (MW)	44.57193	62.56164	70	62.55828	44.61144
P39 (MW)	74.29138	69.58808	100	100	81.36705
P40 (MW)	36.26457	20	20.00006	117.3843	93.68055
P41 (MW)	179.8758	61.06685	180	108.4389	174.218
P42 (MW)	214.8806	170.4508	50	89.75025	200.7572
P43 (MW)	440	434.0589	440	439.9357	440
P44 (MW)	548.9356	560	560	557.9989	553.5239
P45 (MW)	656.1668	660	660	660	659.95
P46 (MW)	619.8882	552.7796	700	652.9989	616.8774
P47 (MW)	7.818483	20.17209	5.4	13.05572	5.435878
P48 (MW)	9.676454	18.31409	5.4	5.409877	7.411779
P49 (MW)	8.668076	43.58376	8.4	30.76577	16.60949
P50 (MW)	8.49503	18.74682	8.4	14.85525	8.816006
P51 (MW)	15.86958	15.03547	8.4	8.710865	14.96421
P52 (MW)	12	12.12576	12	12.03312	15.87253
P53 (MW)	12.58266	26.34686	12	14.22486	12.21051
P54 (MW)	12.99048	12.04599	12	13.86783	12.05828
P55 (MW)	12.01301	12.66599	12	12	13.81338
P56 (MW)	37.17278	26.88475	25.2	72.39573	90.98566
P57 (MW)	37.97543	47.31701	25.2	30.84674	39.52808
P58 (MW)	51.59871	35	35	68.91024	80.72538
P59 (MW)	58.76934	97.12288	35	35.14155	60.09887
P60 (MW)	45.07294	57.22598	45	49.54442	45.67647
P61 (MW)	78.18369	99.98026	45.00001	64.25369	47.63764
P62 (MW)	45.09367	58.11781	45	45.09173	48.00394
P63 (MW)	178.0587	185	54.3	184.8126	143.3335
P64 (MW)	123.7391	58.11555	185	185	107.5385
P65 (MW)	182.4172	172.3989	185	182.2129	167.4087
P66 (MW)	181.6759	54.3	54.3	185	175.4523
P67 (MW)	70.04113	71.52256	70.00001	78.6103	70.38828
P68 (MW)	71.86654	70	70.00004	70	70.76795
P69 (MW)	84.65115	78.06458	70	75.43096	70.37324
P70 (MW)	301.7323	177.1164	360	360	344.8961
P71 (MW)	399.5556	400	400	400	397.789
P72 (MW)	353.6583	394.0654	400	400	397.7459
P73 (MW)	187.6238	155.3777	300	96.81548	192.1567
P74 (MW)	174.1112	200.9273	50.0001	135.8347	222.6639
P75 (MW)	89.89853	90	30	39.41893	42.3146
P76 (MW)	47.07238	50	50	38.22897	30.99924
P77 (MW)	301.436	442.0962	450	310.2392	296.3219
P78 (MW)	389.3647	546.0889	600	525.6255	429.992
P79 (MW)	148.8326	183.8953	200	181.8232	71.24911
P80 (MW)	57.71897	120	120	20	87.21158
P81 (MW)	10.05398	29.67041	10.00019	39.93151	23.65178
P82 (MW)	35.80191	12	12.00092	12.77786	20.41162
P83 (MW)	20.7817	26.57281	80	30.48403	42.34605
P84 (MW)	180.9247	50	200	163.7517	198.0947
P85 (MW)	324.4898	239.2535	325	323.528	276.9616
P86 (MW)	410.1772	296.5789	440	440	427.3867
P87 (MW)	10.00372	35	10	10.00062	13.51488
P88 (MW)	37.53324	30.06295	20.00001	40.25334	53.07498
P89 (MW)	99.17771	89.77608	20.00479	42.95365	22.06654
P90 (MW)	166.7685	201.2848	220	167.7133	173.6614
P91 (MW)	84.46154	30	30	30	120.5089
P92 (MW)	90.56349	100	40	100	93.40121
P93 (MW)	435.4527	440	440	440	439.5659
P94 (MW)	479.4146	493.7429	500	500	428.3421
P95 (MW)	594.4542	600	600	600	600
P96 (MW)	518.1872	634.3845	200	533.8051	505.8276
P97 (MW)	6.887408	8.4532	3.6	3.6	6.877397
P98 (MW)	3.6	6.27438	3.6	3.981924	3.703808
P99 (MW)	4.515441	9.967985	4.4	4.4	4.627253
P100 (MW)	7.624756	4.4	22	4.4	8.498581
P101 (MW)	10.02554	14.08068	60	28.29342	12.21866
P102 (MW)	16.88769	51.89729	10.00006	29.59184	14.49934
P103 (MW)	25.53068	40.51824	20.00569	46.72138	22.5554
P104 (MW)	20.3262	42.66544	20	41.19115	28.56763
P105 (MW)	40.02054	40	40	47.05959	40.29535
P106 (MW)	40.21802	40	40	50.8729	42.39801
P107 (MW)	50.08848	50.80527	50.00001	50.04667	51.08784
P108 (MW)	33.07944	39.38022	30	30.01971	53.22926
P109 (MW)	40.02948	62.98601	40	42.85748	43.88329
P110 (MW)	20.4497	64.54053	20	20	28.91802
V(MW)	1.07E−01	1.73E−01	5.91E−08	1.72E−02	3.54E−03
Fuel Cost ($/h)	200266.5	207194.8	202888.6	202010.7	201505.7

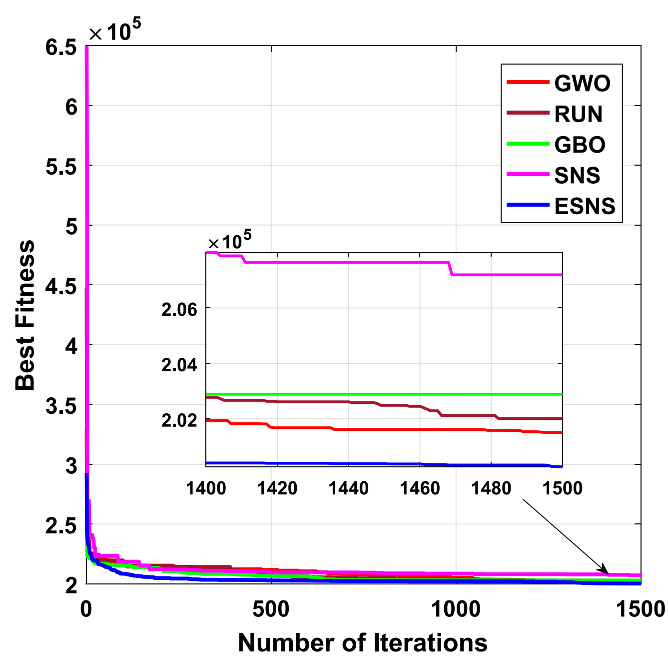

Fig. 15. The convergence curves of the proposed ESNS and other recent algorithms for case 4.

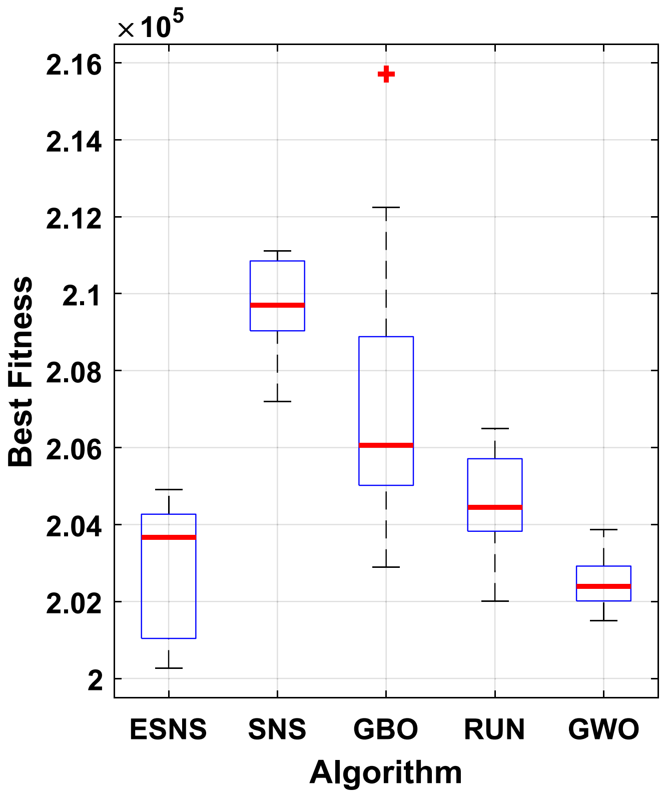

Fig. 16. boxplots of different techniques (Case study 4).

Table 15
the Statistical results of fuel cost using the studied algorithms for Case 4.

Method	Best	Worst	Median	Average	Std.
ESNS	200266.5	202925.5	203669.1	204,908	1669.812
SNS	207194.8	209977.1	209698.1	211106.9	1063.516
GBO	202888.6	207338.9	206063.1	215710.8	3248.177
RUN	202010.7	204777.8	204447.2	206498.3	1205.59
GWO	201505.7	202480.1	202,387	203869.7	598.0938

5. Discussion

The Economic Load Dispatch (ELD) problem is a significant research area in power systems engineering. It involves determining the most efficient distribution of power among generating units in the power system to optimize the overall operating cost of the power system and enhance its efficiency. In this article, four standard test systems, including 11-, 15-, 40-, and 110-unit commonly used in power system studies were used to cover the analyses. The proposed ESNS algorithm is successfully developed and implemented for solving the ELD problem. Section 4 shows the simulation results of the proposed ESNS in two parts to show the superiority and performance of the proposed algorithm. In the first subsection, The performance of ESNS has been tested in the 23 benchmark test suits, and its superiority against SNS and other recent algorithms has been verified. Then, The proposed ESNS was applied to the ELD problems in the second subsection. The proposed ESNS algorithm showed that balancing the exploration and exploitation of this algorithm with high and low-velocity ratio strategy can find the optimum fuel types for each generator and obtain the best power outputs with minimum fuel costs in order to satisfy the load demand in the grid.

Based on the comprehensive analysis of the experimental results presented in Tables 9, 11, 13, and 15, it is unequivocally established that the ESNS algorithm has demonstrated remarkable superiority over its predecessors, including the SNS, GBO, RUN, and GWO algorithms. Furthermore, a comparative evaluation against various state-of-the-art algorithms culled from recent literature corroborates the outstanding performance of the ESNS algorithm in terms of optimizing fuel costs in power systems. One of the key hallmarks of the ESNS algorithm lies in its inherent capability to holistically address intricate constraints encountered in the realm of power system optimization. These constraints encompass generation capacity limitations, transmission losses, and the challenges posed by large-scale systems. This combination of complex constraints is adeptly managed by the ESNS algorithm, which thereby produces solutions of considerably superior quality when compared to its studied algorithms, namely the SNS, GBO, RUN, and GWO algorithms.

The convergence curves of the algorithm in solving the dispatching problems such as in Figs. 5, 7, 9, 11, 13, and 15 for all test systems in all trials show that the convergence normally happens in acceptable iterations. The convergence curves trials of all case study systems show that the convergences are not too early and not too late. Although the final obtained values outperformed other quoted methods, the results could be near optimal values. From the above figures, it is clear that A major feature underlying the ESNS algorithm's prowess is its capacity to achieve enhanced convergence and solution stability when contrasted with the original SNS, GBO, RUN, and GWO algorithms.

It is imperative to note that these insights are gleaned from the meticulous application of the ESNS algorithm to four standard test systems, featuring 11, 15, 40, and 110 units, each characterized by diverse operating constraints. the ESNS's adept handling of complex constraints, superior solution quality, stability, and environmentally conscious optimization converges to position the ESNS algorithm as an indispensable tool in the quest for efficient and sustainable power generation. Moreover, The simulation results obtained from all the cases indicated significant improvements in the system performance and validated the efficacy of the proposed ESNS methodology. The introduction of the proposed algorithm for ELD provides a comprehensive approach to address the challenges associated with determining the most efficient distribution of power among generating units in the power

Table 17
Friedman test for the five algorithms.

Case no.	ESNS	SNS	GBO	RUN	GWO
Case 1	1.05	4.65	2.05	3.2	4.05
Case 2	1	2.95	3.05	3.05	4.95
Case 3	1.75	1.35	4.7	3.85	3.35
Case 4	1.8	4.85	3.8	3.05	1.5
Mean ranks	1.4	3.45	3.4	3.2875	3.4625

Table 16
Statistical results of the Wilcoxon rank-sum test.

ESNS vs	SNS		GBO		RUN		GWO	
Case no.	P	winner	P	winner	P	winner	P	winner
Case 1	6.7956E−08	+	9.2780E−05	+	6.7956E−08	+	6.7956E−08	+
Case 2	6.1266E−08	+	5.2497E−08	+	5.4047E−08	+	5.4600E−08	+
Case 3	5.6517E−02	=	7.8980E−08	+	3.4156E−07	+	3.4156E−07	+
Case 4	6.1529E−08	+	3.0691E−06	+	3.5859E−04	+	2.1841E−01	=
Wilcoxon's ranksum test (+/=/−)	3/1/0		4/0/0		4/0/0		3/1/0	

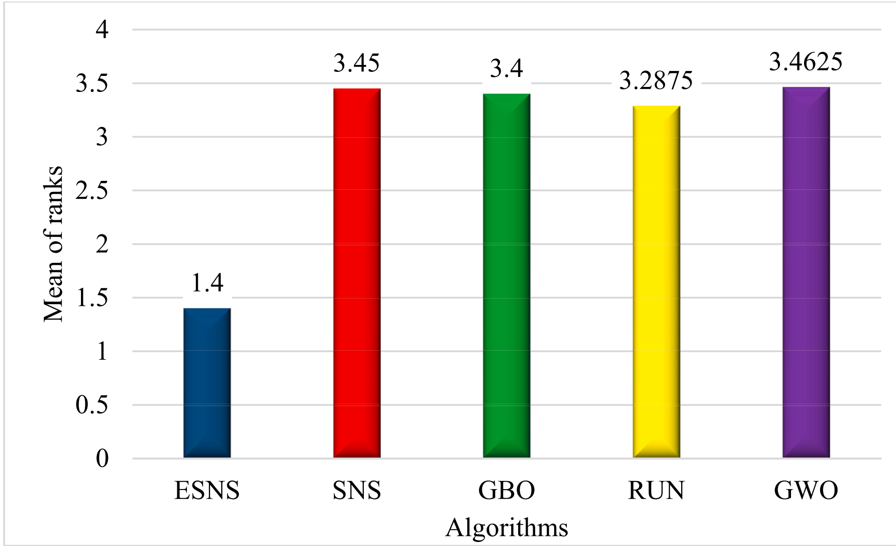

Fig. 17. Mean ranks obtained by Friedman's rank test for four cases using various algorithms.

Table 18
The average CPU time of various algorithms for different test systems.

Number of units	ESNS	SNS	GBO	RUN	GWO
11-unit	85.2942	73.8678	89.8031	136.106	41.8947
15-unit	94.9765	77.4962	99.8369	119.648	48.5059
40-unit	61.4472	52.0543	70.557	109.327	37.2507
110-unit	254.541	201.805	267.084	297.062	144.262

system. It is worth noting that the power system operation costs millions of dollars annually that even a small improvement in the cost reduction and computation can save a large amount of budget. This can be achieved by utilizing the proposed method as an energy management system to handle the economic dispatch of units in the grid.

6. Conclusion

The proposed ESNS algorithm presents a promising solution for the Economic Load Dispatch (ELD) problem, demonstrating its effectiveness in handling the non-convexity, non-drivability, and nonlinearity characteristics of the problem, as well as its ability to address multiple constraints. The validation of the ESNS algorithm involved extensive testing on 23 benchmark functions. The proposed ESNS technique outperforms the SNS, WHO, EO, and JS algorithms. Then, the medium, and large electric power test systems are undertaken to validate the applicability of the proposed technique. It was applied to standard test systems, including 11-, 15-, 40-, and 110-unit systems commonly used in power system studies. To validate the effect of the ESNS technique, the ESNS results were compared with those of the SNS, GBO, RUN, and GWO algorithms. The results obtained from the ESNS algorithm exhibited superior solution quality and convergence speed compared to other optimization algorithms. The ESNS's effective exploration and exploitation of the search space make it a valuable tool for solving the ELD

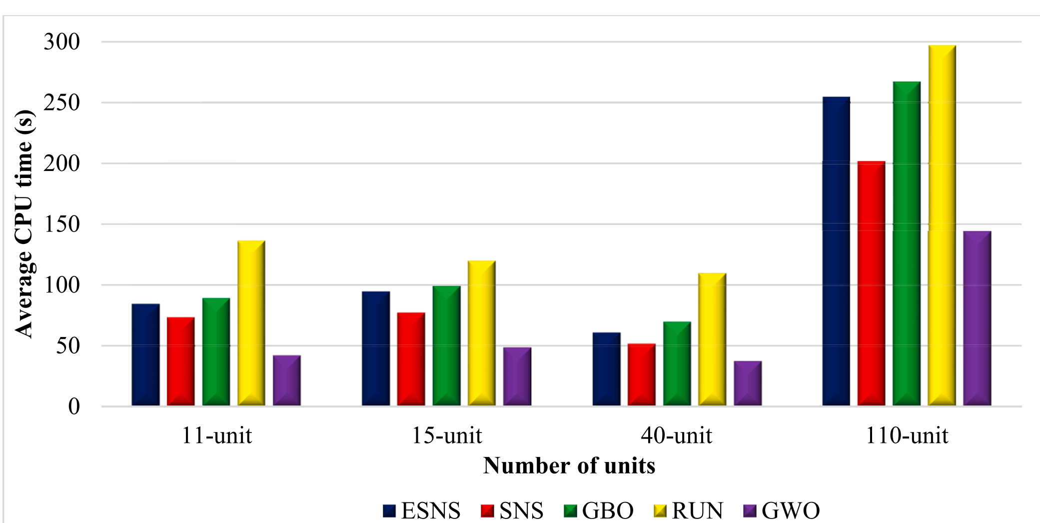

Fig. 18. Average CPU times of various algorithms for different test systems.

problem. The ESNS algorithm offers a robust and efficient solution to the challenging ELD problem, demonstrating its capability to handle various constraints and non-linearities associated with power system economics. Its superior performance compared to other optimization techniques positions it as a promising tool for both researchers and power system operators. The development of the ESNS algorithm showcases the potential of employing innovative and unconventional approaches to tackle complex optimization problems in power system economics. Future work in ELD optimization can explore the application of the ESNS algorithm to larger power systems with increased units and constraints. Assessing the algorithm's scalability in handling larger systems will be crucial for its practical implementation in real-world power systems. Furthermore, additional research can investigate the ESNS algorithm's performance under diverse operating conditions, such as varying load demands and integration of renewable energy sources. This would provide valuable insights into the algorithm's robustness and adaptability to changing system dynamics, further enhancing its applicability and effectiveness in the field of power system optimization.

Declaration of competing interest

The authors declare that they have no known competing financial interests or personal relationships that could have appeared to influence the work reported in this paper.

Data availability

Data will be made available on request.

References

[1] Iqbal MN, Bhatti AR, Butt AD, Sheikh YA, Paracha KN, Ashique RH. Solution of Economic Dispatch Problem Using Hybrid Multi-Verse Optimizer. Electr Pow Syst Res 2022;208:107912. https://doi.org/10.1016/j.epsr.2022.107912.
[2] Hassan MH, Kamel S, Domínguez-García JL, El-Naggar MF. MSSA-DEED: A Multi-Objective Salp Swarm Algorithm for Solving Dynamic Economic Emission Dispatch Problems. Sustainability 2022;14:9785. https://doi.org/10.3390/su14159785.
[3] Ahmed I, Rehan M, Basit A, Malik SH, Alvi U-E-H, Hong K-S. Multi-area economic emission dispatch for large-scale multi-fueled power plants contemplating inter-connected grid tie-lines power flow limitations. Energy 2022;261:125178. Doi: 10.1016/j.energy.2022.125178.
[4] Hassan MH, Kamel S, Eid A, Nasrat L, Jurado F, Elnaggar MF. A developed eagle-strategy supply-demand optimizer for solving economic load dispatch problems. Ain Shams Eng J 2023;14:102083. https://doi.org/10.1016/j.asej.2022.102083.
[5] Gaing Z-L. Particle swarm optimization to solving the economic dispatch considering the generator constraints. IEEE Trans Power Syst 2003;18:1187–95. https://doi.org/10.1109/TPWRS.2003.814889.
[6] Basu M. Modified particle swarm optimization for nonconvex economic dispatch problems. Int J Electr Power Energy Syst 2015;69:304–12. https://doi.org/10.1016/j.ijepes.2015.01.015.
[7] Elsayed WT, Hegazy YG, El-bages MS, Bendary FM. Improved Random Drift Particle Swarm Optimization With Self-Adaptive Mechanism for Solving the Power Economic Dispatch Problem. IEEE Trans Industr Inform 2017;13:1017–26. https://doi.org/10.1109/TII.2017.2695122.
[8] Liu T, Jiao L, Ma W, Ma J, Shang R. Cultural quantum-behaved particle swarm optimization for environmental/economic dispatch. Appl Soft Comput 2016;48:597–611. https://doi.org/10.1016/j.asoc.2016.04.021.
[9] Gholamghasemi M, Akbari E, Asadpoor MB, Ghasemi M. A new solution to the non-convex economic load dispatch problems using phasor particle swarm optimization. Appl Soft Comput 2019;79:111–24. https://doi.org/10.1016/j.asoc.2019.03.038.
[10] Banerjee S, Maity D, Chanda CK. Teaching learning based optimization for economic load dispatch problem considering valve point loading effect. Int J Electr Power Energy Syst 2015;73:456–64. https://doi.org/10.1016/j.ijepes.2015.05.036.
[11] Alzubi I, Al-Masri HMK, Abuelrub A. Modified Particle Swarm Optimization Algorithms for Solving Economic Load Dispatch. In: 2022 3rd International Conference on Smart Grid and Renewable Energy (SGRE), IEEE; 2022. p. 1–5. https://doi.org/10.1109/SGRE53517.2022.9774126.
[12] Pan J, Shan J, Chu S, Jiang S, Zheng S, Liao L. A multigroup marine predator algorithm and its application for the power system economic load dispatch. Energy Sci Eng 2022;10:1840–54. https://doi.org/10.1002/ese3.957.
[13] Bhattacharjee K, Patel N. A comparative study of Economic Load Dispatch with complex non-linear constraints using Salp Swarm Algorithm. Sci Iran 2020. https://doi.org/10.24200/sci.2020.52145.2562.
[14] Economic BK, Optimization DPUBS. Int J Energy Optim Eng 2018;7:39–60. https://doi.org/10.4018/IJEOE.2018040102.
[15] Hassan MH, Kamel S, Abualigah L, Eid A. Development and application of slime mould algorithm for optimal economic emission dispatch. Expert Syst Appl 2021;182:115205. https://doi.org/10.1016/j.eswa.2021.115205.
[16] Singh T. Chaotic slime mould algorithm for economic load dispatch problems. Appl Intell 2022;52:15325–44. https://doi.org/10.1007/s10489-022-03179-y.
[17] Fu L, Ouyang H, Zhang C, Li S, Mohamed AW. A constrained cooperative adaptive multi-population differential evolutionary algorithm for economic load dispatch problems. Appl Soft Comput 2022;121:108719. https://doi.org/10.1016/j.asoc.2022.108719.
[18] Kaboli SHrA, Alqallaf AK. Solving non-convex economic load dispatch problem via artificial cooperative search algorithm. Expert Syst Appl 2019;128:14–27. Doi: 10.1016/j.eswa.2019.02.002.
[19] Basu M. Fast convergence evolutionary programming for economic dispatch problems. IET Gener Transm Distrib 2017;11:4009–17. https://doi.org/10.1049/iet-gtd.2017.0275.
[20] Kamboj VK, Bhadoria A, Bath SK. Solution of non-convex economic load dispatch problem for small-scale power systems using ant lion optimizer. Neural Comput Appl 2017;28:2181–92. https://doi.org/10.1007/s00521-015-2148-9.
[21] Nguyen TT, Vo DN. The application of one rank cuckoo search algorithm for solving economic load dispatch problems. Appl Soft Comput 2015;37:763–73. https://doi.org/10.1016/j.asoc.2015.09.010.
[22] Secui DC. A modified Symbiotic Organisms Search algorithm for large scale economic dispatch problem with valve-point effects. Energy 2016;113:366–84. https://doi.org/10.1016/j.energy.2016.07.056.
[23] Bhattacharjee K, Bhattacharya A, Dey SH nee. Oppositional Real Coded Chemical Reaction Optimization for different economic dispatch problems. Int J Electr Power Energy Syst 2014;55:378–91. https://doi.org/10.1016/j.ijepes.2013.09.033.
[24] Zakian P, Kaveh A. Economic dispatch of power systems using an adaptive charged system search algorithm. Appl Soft Comput 2018;73:607–22. https://doi.org/10.1016/j.asoc.2018.09.008.
[25] Bhattacharjee K, Bhattacharya A, Halder nee Dey S. Chemical reaction optimisation for different economic dispatch problems. IET Generation, Transmission & Distribution 2014;8:530–41. Doi: 10.1049/iet-gtd.2013.0122.
[26] Elsakaan AA, El-Sehiemy RA, Kaddah SS, Elsaid MI. An enhanced moth-flame optimizer for solving non-smooth economic dispatch problems with emissions. Energy 2018;157:1063–78. https://doi.org/10.1016/j.energy.2018.06.088.
[27] Bhattacharjee K, Patel N. An experimental study regarding Economic Load Dispatch using Search Group Optimization. Sci Iran 2019. https://doi.org/10.24200/sci.2019.51798.2367.
[28] Cui S, Wang Y-W, Lin X, Liu X-K. Distributed auction optimization algorithm for the nonconvex economic dispatch problem based on the gossip communication mechanism. Int J Electr Power Energy Syst 2018;95:417–26. https://doi.org/10.1016/j.ijepes.2017.09.012.
[29] Srivastava A, Das DK. A new Kho-Kho optimization Algorithm: An application to solve combined emission economic dispatch and combined heat and power economic dispatch problem. Eng Appl Artif Intell 2020;94:103763. https://doi.org/10.1016/j.engappai.2020.103763.
[30] Singh D, Dhillon JS. Ameliorated grey wolf optimization for economic load dispatch problem. Energy 2019;169:398–419. https://doi.org/10.1016/j.energy.2018.11.034.
[31] Sun J, Deng J, Li Y. Indicator & crowding distance-based evolutionary algorithm for combined heat and power economic emission dispatch. Appl Soft Comput 2020;90:106158. https://doi.org/10.1016/j.asoc.2020.106158.
[32] Ghasemi M, Taghizadeh M, Ghavidel S, Abbasian A. Colonial competitive differential evolution: An experimental study for optimal economic load dispatch. Appl Soft Comput 2016;40:342–63. https://doi.org/10.1016/j.asoc.2015.11.033.
[33] Ghasemi M, Ghavidel S, Aghaei J, Akbari E, Li L. CFA optimizer: A new and powerful algorithm inspired by Franklin's and Coulomb's laws theory for solving the economic load dispatch problems. Int Trans Elect Energy Syst 2018;28:e2536.
[34] Mohammadi F, Abdi H. A modified crow search algorithm (MCSA) for solving economic load dispatch problem. Appl Soft Comput 2018;71:51–65. https://doi.org/10.1016/j.asoc.2018.06.040.
[35] Yu J, Kim C-H, Rhee S-B. Clustering cuckoo search optimization for economic load dispatch problem. Neural Comput Appl 2020;32:16951–69. https://doi.org/10.1007/s00521-020-05036-w.
[36] Prakash T, Singh VP, Singh SP, Mohanty SR. Economic load dispatch problem: quasi-oppositional self-learning TLBO algorithm. Energy Syst 2018;9:415–38. https://doi.org/10.1007/s12667-017-0230-3.
[37] Pattanaik JK, Basu M, Dash DP. Dynamic economic dispatch: a comparative study for differential evolution, particle swarm optimization, evolutionary programming, genetic algorithm, and simulated annealing. J Electr Syst Inf Technol 2019;6:1. https://doi.org/10.1186/s43067-019-0001-4.
[38] Sharifian Y, Abdi H. Solving multi-area economic dispatch problem using hybrid exchange market algorithm with grasshopper optimization algorithm. Energy 2023;267:126550. https://doi.org/10.1016/j.energy.2022.126550.
[39] Al-Betar MA, Awadallah MA, Makhadmeh SN, Doush IA, Zitar RA, Alshathri S, et al. A hybrid Harris Hawks optimizer for economic load dispatch problems. Alex Eng J 2023;64:365–89. https://doi.org/10.1016/j.aej.2022.09.010.
[40] Braik M, Awadallah MA, Al-Betar MA, Hammouri AI. A hybrid capuchin search algorithm with gradient search algorithm for economic dispatch problem. Soft Comput 2023. https://doi.org/10.1007/s00500-023-09019-6.
[41] Kumar M, Dhillon JS. Hybrid artificial algae algorithm for economic load dispatch. Appl Soft Comput 2018;71:89–109. https://doi.org/10.1016/j.asoc.2018.06.035.
[42] Jayabarathi T, Raghunathan T, Adarsh BR, Suganthan PN. Economic dispatch using hybrid grey wolf optimizer. Energy 2016;111:630–41. https://doi.org/10.1016/j.energy.2016.05.105.

[43] Chansareewittaya S. Hybrid MODE/TS for Environmental Dispatch and Economic Dispatch. ECTI Trans Elect Engi, Electron, Commun 2019;17:78–86. https://doi.org/10.37936/ecti-eec.2019171.215439.

[44] Alkoffash MS, Awadallah MA, Alweshah M, Zitar RA, Assaleh K, Al-Betar MA. A Non-convex Economic Load Dispatch Using Hybrid Salp Swarm Algorithm. Arab J Sci Eng 2021;46:8721–40. https://doi.org/10.1007/s13369-021-05646-z.

[45] Silva Chavez JC, Zamora-Mendez A, Arrieta Paternina MR, Yrena Heredia JF, Cardenas-Javier R. A hybrid optimization framework for the non-convex economic dispatch problem via meta-heuristic algorithms. Electr Pow Syst Res 2019;177: 105999. https://doi.org/10.1016/j.epsr.2019.105999.

[46] Ghasemi M, Aghaei J, Akbari E, Ghavidel S, Li L. A differential evolution particle swarm optimizer for various types of multi-area economic dispatch problems. Energy 2016;107:182–95. https://doi.org/10.1016/j.energy.2016.04.002.

[47] Neto JXV, Reynoso-Meza G, Ruppel TH, Mariani VC, Coelho L dos S. Solving non-smooth economic dispatch by a new combination of continuous GRASP algorithm and differential evolution. Int J Electr Power Energy Syst 2017;84:13–24. https://doi.org/10.1016/j.ijepes.2016.04.012.

[48] Xin-gang Z, Ji L, Jin M, Ying Z. An improved quantum particle swarm optimization algorithm for environmental economic dispatch. Expert Syst Appl 2020;152: 113370. https://doi.org/10.1016/j.eswa.2020.113370.

[49] Ghasemi M, Davoudkhani IF, Akbari E, Rahimnejad A, Ghavidel S, Li L. A novel and effective optimization algorithm for global optimization and its engineering applications: Turbulent Flow of Water-based Optimization (TFWO). Eng Appl Artif Intell 2020;92:103666. https://doi.org/10.1016/j.engappai.2020.103666.

[50] El-Dabah MA, Hassan MH, Kamel S, Zawbaa HM. Robust Parameters Tuning of Different Power System Stabilizers Using a Quantum Artificial Gorilla Troops Optimizer. IEEE Access 2022;10:82560–79. https://doi.org/10.1109/ACCESS.2022.3195892.

[51] Talatahari S, Bayzidi H, Saraee M. Social Network Search for Global Optimization. IEEE Access 2021;9:92815–63. https://doi.org/10.1109/ACCESS.2021.3091495.

[52] El-Sehiemy R, Elsayed A, Shaheen A, Elattar E, Ginidi A. Scheduling of Generation Stations, OLTC Substation Transformers and VAR Sources for Sustainable Power System Operation Using SNS Optimizer. Sustainability 2021;13:11947. https://doi.org/10.3390/su132111947.

[53] Shaheen A, El-Sehiemy R, Kamel S, Selim A. Reliability Improvement Based Reconfiguration of Distribution Networks via Social Network Search Algorithm. 2022 23rd International Middle East Power Systems Conference (MEPCON), IEEE; 2022, p. 1–6. Doi: 10.1109/MEPCON55441.2022.10021721.

[54] Bayzidi H, Talatahari S, Saraee M, Lamarche C-P. Social Network Search for Solving Engineering Optimization Problems. Comput Intell Neurosci 2021;2021: 1–32. https://doi.org/10.1155/2021/8548639.

[55] Sarhan S, Shaheen A, El-Sehiemy R, Gafar M. An Augmented Social Network Search Algorithm for Optimal Reactive Power Dispatch Problem. Mathematics 2023;11:1236. https://doi.org/10.3390/math11051236.

[56] Ahmed I, Rehan M, Basit A, Malik SH, Alvi UEH, Hong KS. Multi-area economic emission dispatch for large-scale multi-fueled power plants contemplating inter-connected grid tie-lines power flow limitations. Energy 2022;261:125178. https://doi.org/10.1016/j.energy.2022.125178.

[57] Hassan MH, Houssein EH, Mahdy MA, Kamel S. An improved Manta ray foraging optimizer for cost-effective emission dispatch problems. Eng Appl Artif Intell 2021; 100:104155. https://doi.org/10.1016/j.engappai.2021.104155.

[58] Faramarzi A, Heidarinejad M, Mirjalili S, Gandomi AH. Marine Predators Algorithm: A nature-inspired metaheuristic. Expert Syst Appl 2020;152:113377. https://doi.org/10.1016/j.eswa.2020.113377.

[59] Naruei I, Keynia F. Wild horse optimizer: a new meta-heuristic algorithm for solving engineering optimization problems. Eng Comput 2022;38:3025–56. https://doi.org/10.1007/s00366-021-01438-z.

[60] Faramarzi A, Heidarinejad M, Stephens B, Mirjalili S. Equilibrium optimizer: A novel optimization algorithm. Knowl Based Syst 2020;191:105190. https://doi.org/10.1016/j.knosys.2019.105190.

[61] Chou J-S, Truong D-N. A novel metaheuristic optimizer inspired by behavior of jellyfish in ocean. Appl Math Comput 2021;389:125535. https://doi.org/10.1016/j.amc.2020.125535.

[62] Wang L, Cao Q, Zhang Z, Mirjalili S, Zhao W. Artificial rabbits optimization: A new bio-inspired meta-heuristic algorithm for solving engineering optimization problems. Eng Appl Artif Intell 2022;114:105082. https://doi.org/10.1016/j.engappai.2022.105082.

[63] Wang Y, Wang P, Zhang J, Cui Z, Cai X, Zhang W, et al. A Novel Bat Algorithm with Multiple Strategies Coupling for Numerical Optimization. Mathematics 2019;7: 135. https://doi.org/10.3390/math7020135.

[64] Kumar A, Wu G, Ali MZ, Mallipeddi R, Suganthan PN, Das S. A test-suite of non-convex constrained optimization problems from the real-world and some baseline results. Swarm Evol Comput 2020;56:100693. https://doi.org/10.1016/j.swevo.2020.100693.

[65] Xue J, Shen B. Dung beetle optimizer: a new meta-heuristic algorithm for global optimization. J Supercomput 2022. https://doi.org/10.1007/s11227-022-04959-6.

[66] Mohammed H, Rashid T. FOX: a FOX-inspired optimization algorithm. Appl Intell 2022. https://doi.org/10.1007/s10489-022-03533-0.

[67] Zhao W, Wang L, Mirjalili S. Artificial hummingbird algorithm: A new bio-inspired optimizer with its engineering applications. Comput Methods Appl Mech Eng 2022; 388:114194. https://doi.org/10.1016/j.cma.2021.114194.

[68] Ahmadianfar I, Heidari AA, Gandomi AH, Chu X, Chen H. RUN beyond the metaphor: An efficient optimization algorithm based on Runge Kutta method. Expert Syst Appl 2021;181:115079. https://doi.org/10.1016/j.eswa.2021.115079.

[69] Mirjalili S, Mirjalili SM, Lewis A. Grey Wolf Optimizer. Adv Eng Softw 2014;69: 46–61. https://doi.org/10.1016/j.advengsoft.2013.12.007.

[70] Ahmadianfar I, Bozorg-Haddad O, Chu X. Gradient-based optimizer: A new metaheuristic optimization algorithm. Inf Sci (N Y) 2020;540:131–59. https://doi.org/10.1016/j.ins.2020.06.037.

[71] Hassan MH, Kamel S, Salih SQ, Khurshaid T, Ebeed M. Developing Chaotic Artificial Ecosystem-Based Optimization Algorithm for Combined Economic Emission Dispatch. IEEE Access 2021;9:51146–65. https://doi.org/10.1109/ACCESS.2021.3066914.

[72] Hassan MH, Kamel S, Jurado F, Ebeed M, Elnaggar MF. Economic load dispatch solution of large-scale power systems using an enhanced beluga whale optimizer. Alex Eng J 2023;72:573–91. https://doi.org/10.1016/j.aej.2023.04.002.

[73] Al-Betar MA, Awadallah MA, Zitar RA, Assaleh K. Economic load dispatch using memetic sine cosine algorithm. J Ambient Intell Humaniz Comput 2022. https://doi.org/10.1007/s12652-022-03731-1.

[74] Huang Z, Zhao J, Qi L, Gao Z, Duan H. Comprehensive learning cuckoo search with chaos-lambda method for solving economic dispatch problems. Appl Intell 2020; 50:2779–99. https://doi.org/10.1007/s10489-020-01654-y.

[75] Safari A, Shayeghi H. Iteration particle swarm optimization procedure for economic load dispatch with generator constraints. Expert Syst Appl 2011;38: 6043–8. https://doi.org/10.1016/j.eswa.2010.11.015.

[76] Sudhakaran M, Ajay-D-Vimalraj P, Palanivelu TG. GA and PSO culled hybrid technique for economic dispatch problem with prohibited operating zones. J Zhejiang Univ-Sci A 2007;8:896–903. https://doi.org/10.1631/jzus.2007.A0896.

[77] Panigrahi BK, Ravikumar PV. Bacterial foraging optimisation: Nelder-Mead hybrid algorithm for economic load dispatch. IET Gener Transm Distrib 2008;2:556. https://doi.org/10.1049/iet-gtd:20070422.

[78] Panigrahi BK, Pandi VR, Das S, Cui Z, Sharma R. Economic load dispatch using population-variance harmony search algorithm. Trans Inst Meas Control 2012;34: 746–54.

[79] Chaturvedi KT, Pandit M, Srivastava L. Self-Organizing Hierarchical Particle Swarm Optimization for Nonconvex Economic Dispatch. IEEE Trans Power Syst 2008;23:1079–87. https://doi.org/10.1109/TPWRS.2008.926455.

[80] Agnihotri S, Atre A, Verma HK. Equilibrium Optimizer for Solving Economic Dispatch Problem. 2020 IEEE 9th Power India International Conference (PIICON), IEEE; 2020, p. 1–5. Doi: 10.1109/PIICON49524.2020.9113048.

[81] Nayak SK, Krishnanand KR, Panigrahi BK, Rout PK. Application of Artificial Bee Colony to economic load dispatch problem with ramp rate limits and prohibited operating zones. 2009 World Congress on Nature & Biologically Inspired Computing (NaBIC), IEEE; 2009, p. 1237–42. Doi: 10.1109/NABIC.2009.5393751.

[82] Yang X-S, Sadat Hosseini SS, Gandomi AH. Firefly Algorithm for solving non-convex economic dispatch problems with valve loading effect. Appl Soft Comput 2012;12:1180–6. https://doi.org/10.1016/j.asoc.2011.09.017.

[83] Barati H, Sadeghi M. An efficient hybrid MPSO-GA algorithm for solving non-smooth/non-convex economic dispatch problem with practical constraints. Ain Shams Eng J 2018;9:1279–87. https://doi.org/10.1016/j.asej.2016.08.008.

[84] Atre A, Agnihotri S, Verma HK. Hybrid EO-SCA Based Economic Load Dispatch. In: 2020 IEEE First International Conference on Smart Technologies for Power, Energy and Control (STPEC). IEEE; 2020. p. 1–6. https://doi.org/10.1109/STPEC49749.2020.9297737.

[85] Ghorbani N, Vakili S, Babaei E, Sakhavati A. Particle swarm optimization with smart inertia factor for solving non-convex economic load dispatch problems. Int Trans Elect Energy Syst 2014;24:1120–33. https://doi.org/10.1002/etep.1766.

[86] Ciornei I, Kyriakides E. A GA-API Solution for the Economic Dispatch of Generation in Power System Operation. IEEE Trans Power Syst 2012;27:233–42. https://doi.org/10.1109/TPWRS.2011.2168833.

[87] Abdullah MN, Abu Bakar AH, Rahim NA, Moklis H. Economic load dispatch with nonsmooth cost functions using evolutionary particle swarm optimization. IEEJ Trans Electr Electron Eng 2013;8:S30–7. https://doi.org/10.1002/tee.21915.

[88] Aragón VS, Esquivel SC, Coello Coello CA. An immune algorithm with power redistribution for solving economic dispatch problems. Inf Sci (N Y) 2015;295: 609–32. https://doi.org/10.1016/j.ins.2014.10.026.

[89] Ghorbani N, Babaei E. Exchange market algorithm for economic load dispatch. Int J Electr Power Energy Syst 2016;75:19–27. https://doi.org/10.1016/j.ijepes.2015.08.013.

[90] Jadhav HT, Roy R. Gbest guided artificial bee colony algorithm for environmental/economic dispatch considering wind power. Expert Syst Appl 2013;40:6385–99. https://doi.org/10.1016/j.eswa.2013.05.048.

[91] Bhattacharjee K, Bhattacharya A, nee Dey SH. Teaching Learning Based Optimization for Different Economic Dispatch Problems. International. J Sci Technol 2014;21:870–84.

[92] Yu J, Kim C-H, Wadood A, Khurshaid T, Rhee S-B. Jaya Algorithm With Self-Adaptive Multi-Population and Lévy Flights for Solving Economic Load Dispatch Problems. IEEE Access 2019;7:21372–84. https://doi.org/10.1109/ACCESS.2019.2899043.

[93] Khamsawang S, Jiriwibhakorn S. DSPSO–TSA for economic dispatch problem with nonsmooth and noncontinuous cost functions. Energy Convers Manag 2010;51: 365–75. https://doi.org/10.1016/j.enconman.2009.09.034.